

Has SUSY Gone Undetected in 9-jet Events? A Ten-Fold Enhancement in the LHC Signal Efficiency

Tianjun Li,^{1,2} James A. Maxin,² Dimitri V. Nanopoulos,^{2,3,4} and Joel W. Walker⁵

¹*Key Laboratory of Frontiers in Theoretical Physics, Institute of Theoretical Physics,
Chinese Academy of Sciences, Beijing 100190, P. R. China*

²*George P. and Cynthia W. Mitchell Institute for Fundamental Physics and Astronomy,
Texas A&M University, College Station, TX 77843, USA*

³*Astroparticle Physics Group, Houston Advanced Research Center (HARC), Mitchell Campus, Woodlands, TX 77381, USA*

⁴*Academy of Athens, Division of Natural Sciences,
28 Panepistimiou Avenue, Athens 10679, Greece*

⁵*Department of Physics, Sam Houston State University, Huntsville, TX 77341, USA*

On the heels of the first analysis of LHC data eclipsing the inverse femtobarn integrated luminosity milestone, we undertake a detailed comparison of the most recent experimental results with Monte Carlo simulation of the full “bare-minimally constrained” parameter space of the class of supersymmetric models which go by the name of No-Scale \mathcal{F} - $SU(5)$. We establish the first sparticle exclusion boundaries on these models, finding that the LSP mass should be at least about 92 GeV, with a corresponding boundary gaugino mass $M_{1/2}$ above about 485 GeV. In contrast to the higher mass constraints established for the CMSSM, we find the minimum exclusion boundary on the \mathcal{F} - $SU(5)$ gluino and heavy squark masses resides in the range of 658-674 GeV and 854-1088 GeV, respectively, with a minimum light stop squark mass of about 520 GeV. Moreover, we show that elements of the surviving parameter space not only escape the onslaught of LHC data which is currently decimating the standard mSUGRA/CMSSM benchmarks, but are further able to *efficiently explain* certain tantalizing production excesses over the SM background which have been reported by the CMS collaboration. We also extend this study comparatively to five distinct collider energies and four specific cut methodologies, including a proposed set of selection cuts designed to reveal the natural ultra-high jet multiplicity signal associated with the stable mass hierarchy $m_{\tilde{t}} < m_{\tilde{g}} < m_{\tilde{q}}$ of the \mathcal{F} - $SU(5)$ models. By so doing, we demonstrate that a rather stable enhancement in model visibility, conservatively of order ten, may be attained by adoption of these cuts, which is sufficient for an immediate and definitive testing of a majority of the model space using only the existing LHC data set. We stress the point that habits established in lower jet multiplicity searches do not necessarily carry over into the ultra-high jet multiplicity search regime.

PACS numbers: 11.10.Kk, 11.25.Mj, 11.25.-w, 12.60.Jv

I. INTRODUCTION AND MOTIVATION

The task given to experimentalists is one of exceeding difficulty, and the position of the goalposts is in constant flux. Yesterday’s sensation is tomorrow’s calibration, as the maxim goes, and signals not long ago heralded simply for the seeing, come soon to be reclassified as background, and must become sufficiently well resolved that they may be seen *past*. Seeking out the tails of statistical distribution tails, the right tool is essential. If one wishes to find needles in a haystack, a magnet may prove more useful than a pitchfork. No one much doubts that the LHC is a suitable tool, or that the forthcoming energy doubling to $\sqrt{s} = 14$ TeV will make it ever much more so, and indeed many times more so than twice. However, there are certain complementary tools in the experimental arsenal which may be deployed for a cost somewhat less than US \$10 billion.

The most significant such tool is the data selection cut. Simply speaking, one must isolate, or select, potential outcomes which are accessible to the desired signal, but inaccessible to, or at least substantially unlikely for, the competing background. It may actually be beneficial to discard even a large quantity of signal events

from regions of phase space which are background dominated, in favor of a smaller quantity of retained events of an unusual character which may be uniquely differentiated. A second layer of selection filtering may typically be applied to eliminate faked signals attributable to the persistent incompleteness and occasional fallibility of detector measurements. Careful tailoring of the cuts to the sought signal may readily account for orders of magnitude of relative signal enhancement, and great effort is thus expended in this pursuit, commensurate with the weight of potential benefit that the cuts employed may leverage against the great cost and effort of the project at large.

Cuts highly specialized for a single given task are though not guaranteed to be suitable for any secondary purpose, and worse, may in fact mask or obscure the detection of alternatively feasible physical models. The cuts featured most prominently in the early LHC studies are geared toward evocation of minimal supergravity (mSUGRA) and the Constrained Minimal Supersymmetric Standard Model (CMSSM). This is neither surprising nor unreasonable; chasing plurality without necessity is a fool’s errand. However, the moment of escalation may be at hand with the recent announcement that a definitive

marker of supersymmetry (SUSY) at the LHC escapes the scrutiny of the first complete inverse femtobarn of integrated luminosity [1]. It was concluded by one particular study [2], based on just the first 165 pb^{-1} of data, that more than 99% of the minimal parameter space had been already disfavored, and similarly dire pronouncements, claiming an even greater scope, may be expected to follow the most recently reported results. Most significantly, as exclusion boundaries on heavy squarks creep above the TeV level, the very *raison d'être* of SUSY itself becomes imperiled; as a solution to the stabilization of the gauge hierarchy of the electroweak scales, and as an appeal to naturalness against the spectre of fine tuning, SUSY should embody sparticle mass splittings which are not greater than the range of several hundreds of GeV, or at most about one TeV.

In the present work, we will perform an explicit comparison of the model space of a construction dubbed No-Scale \mathcal{F} - $SU(5)$ against the most recently reported experimental results, establishing the first sparticle mass limits which apply to these models, and emphasizing that, by mimicking the published CMS cutting methodology, we may further efficiently account within the remaining parameter space for the statistical excesses (though insufficient for formal discovery) which have been observed above the Standard Model (SM) expectation [1]. We will then proceed by detailed steps toward the central conclusion of our current analysis, namely that the No-Scale \mathcal{F} - $SU(5)$ model experiences on the order of a ten-fold enhancement in visibility, and possibly even substantially more, by the application of cuts tuned to its distinctive ultra-high jet signal; this enhancement is more than sufficient to claim immediate SUSY discovery within large portions of the model, using only the existing data accumulation.

Whether this specific model should ultimately be shown to be correct or incorrect, it serves here nonetheless as an immediate and practical warning against any misconception that limits currently being established by the ATLAS and CMS collaborations within the mSUGRA/CMSSM context may be globally extrapolated onto the underlying framework of SUSY itself. A more comprehensive probe of the SUSY model space will necessarily entail application of a wider variety of selection criteria against the wealth of accumulated raw data. After all, we remind the reader that CMS does indeed still stand for “Compact Muon Solenoid”, and most certainly not for “Constrained Minimal Supersymmetry”.

II. FOUNDATIONS OF NO-SCALE \mathcal{F} - $SU(5)$

Recently, we have studied in some substantial detail a model by the name of No-Scale \mathcal{F} - $SU(5)$ [3–12], constructed upon the tri-podal foundation of the \mathcal{F} -lipped $SU(5)$ Grand Unified Theory (GUT) [13–15], two pairs of hypothetical TeV scale vector-like SUSY multiplets with origins in \mathcal{F} -theory [16–20], and the dynamically estab-

lished boundary conditions of No-Scale Supergravity [21–25]. For a more complete review, the reader is directed to the appendix of Ref. [8], and to the references therein.

An accumulating body of work argues that the speculative components of No-Scale \mathcal{F} - $SU(5)$ offer actually a clear path toward reduced plurality in postulate, via the singularly natural treatment of such disparate concerns as radiative electroweak symmetry breaking (EWSB) [26] and stabilization of the gauge hierarchy, precision coupling unification [27–32]¹ and reconciliation of the “little hierarchy” between the GUT and Planck scales [16, 19, 34], suppression of dimension five proton decay by colored Higgsino exchange [15], electroweak doublet-triplet splitting by the missing partner mechanism [15], a neutralino cold dark matter (CDM) candidate [35–37], appropriately small seesaw neutrino masses [38–40], chiral GUT higgs representations and gauge symmetry breaking by flux activation [17, 18, 41–45], realization of the gravitational decoupling scenario [17, 18], narrow refinement of the electroweak (EW) Higgs vacuum expectation value (VEV) ratio $\tan \beta$, the dynamic origin of a single SUSY breaking mass, cosmological flatness [21], and the monopole problem, all within a framework granted the *imprimatur* of a string motivated origination.

The model demonstrates a high precision of predictive constraint, especially in the relatively narrow parameterization freedom of the SUSY sparticle sector, as enforced by the No-Scale boundary conditions, and in particular, the non-trivial vanishing of the Higgs bilinear soft term B_μ at the high scale. Notably, this scenario appears to come into its own only when applied at an elevated scale, approaching the Planck mass [46, 47]. Likewise, $M_{\mathcal{F}}$, the point of the second stage flipped $SU(5) \times U(1)_X$ unification, emerges in turn as a suitable candidate scale only when substantially decoupled from the primary GUT scale unification of $SU(3)_C \times SU(2)_L$ via the modification to the renormalization group equations (RGEs) from the extra \mathcal{F} -theory vector multiplets [3, 4]. This interdependence highlights the mutually essential roles of the three foundational postulates, and the manner by which they conspire to reduce rather than enlarge the level of uncertainty in the model’s predicted phenomenology.

We will here show that regions of the bare-minimally constrained [9] parameter space of No-Scale \mathcal{F} - $SU(5)$, simultaneously consistent with the measured top-quark mass m_t , the No-Scale boundary conditions, radiative EWSB, the centrally observed WMAP7 CDM relic density [48], and precision LEP constraints on the lightest CP-even Higgs boson m_h [49, 50] and other light SUSY chargino and neutralino mass content, remain viable even after announcement of the upgraded LHC data sets. The most favorable regions that include secondary bounds on the flavor changing neutral current ($b \rightarrow s\gamma$) pro-

¹ Such precise gauge unification does not occur in non-supersymmetric $SU(5)$ [33]

cess and on contributions to the muon anomalous magnetic moment $(g - 2)_\mu$ are automatically satisfied for at least regional intersections within this space, while limits on the rare decay $B_s^0 \rightarrow \mu^+ \mu^-$ [51] are satisfied for the entire model space, all of which is moreover consistent with spin-independent [52] and spin-dependent [53] scattering cross-section bounds on Weakly Interacting Massive Particles (WIMPs), and ongoing collider searches for a Higgs signal. We attribute this remarkable survival chiefly to the characteristically stable sparticle mass hierarchy $m_{\tilde{t}} < m_{\tilde{g}} < m_{\tilde{q}}$ of a light stop and gluino, both comfortably lighter than all other squarks. This hierarchy allows No-Scale \mathcal{F} - $SU(5)$ to evade collider limits on light squark masses much more nimbly than CMSSM constructions with comparably light Lightest Supersymmetric Particles (LSPs).

Most critically, this convergence of theoretical efficiency, tight predictive constraint, and adroit evasion of the crossfire of current experimental results, is further coupled, somewhat paradoxically, to an encompassing air of imminent testability. No-Scale \mathcal{F} - $SU(5)$ has escaped the advancing LHC exclusions not by being vague or by making predictions which are inaccessible to contemporary search capabilities, but rather by hiding in plain sight. The full parameter space features a dominantly Bino LSP at a purity greater than 99.7%, which is automatically safe with respect to existing DM direct detection searches, as led by the XENON100 [52] collaboration, yet well positioned for a near-term shot at the discovery and classification of a CDM candidate [10]. With regards to the LHC collider effort, the same properties of the sparticle mass hierarchy which cause No-Scale \mathcal{F} - $SU(5)$ to fare rather poorly under conventional search strategies simultaneously affords a stably definitive collider signal of ultra-high multiplicity jet events [7, 8] which yields a dramatic resonant enhancement in visibility under selection cuts tuned to its own peculiar character. This latter point will be supported by the detailed demonstration that adoption of a non-standard ultra-high jet multiplicity selection criteria can yield on the order of a ten times enhancement in the detection efficiency of No-Scale \mathcal{F} - $SU(5)$, within the existing physical constraints of the collider apparatus.

Like Michelangelo’s David, ensconced still by raw marble before application of the hammer and chisel, our prize may stand already before us; all we need yet do is cut away that which is not David.

III. NO-SCALE \mathcal{F} - $SU(5)$ IN THE LIGHT OF A 1.1 fb^{-1} INTEGRATED LUMINOSITY

A primary concern accompanying the release of a substantially upgraded quantity of data which probes post-SM physics with unprecedented energy resolution is whether or not one’s preferred model has survived the search. A secondary, though entangled, question is whether one’s preferred model may in fact have been

glimpsed, even perhaps faintly, peeking over the background. We first attempted to mimic an earlier generation of the cuts favored by the CMS collaboration [54, 55] in Refs. [7, 8]. The detailed selection criteria employed are summarized in Table (II) of Ref. [8] and the surrounding discourse of Section (IV). For simplicity, both there and here, we describe the standard intermediate jet count searches in shorthand to be of the “CMS” style, although our discussion is obviously of equal relevance to the sister ATLAS detector. We presently implement a few minor updates to the original “CMS” cuts, designed to mirror the most recently presented collaboration physics analysis summary [1]. In particular, we are adjusting the lower bounds of 350 GeV and 150 GeV on the net scalar sum of transverse momentum H_T and the missing transverse energy H_T^{miss} to 375 GeV and 100 GeV, respectively. Although the CMS collaboration now more broadly advocates a larger quantity of individual H_T bins, starting at 275, with individually tuned thresholds on the transverse momentum p_T per jet in the lower two bins, a useful presentation of the observed signal and background calibration is presented in Section (2.1) of Ref. [1] with the single $H_T \geq 375$ GeV cut, which we shall for simplicity follow. Additionally, the maximal pseudo-rapidity η of the leading jet has been raised from 2.0 to 2.5, although the threshold of 3.0 for sub-leading jets remains fixed.

Other selection criteria generally remain in place, including a lower bound of 50 GeV for the transverse momentum p_T of each hard jet, an upper bound of 0.9 on the the electromagnetic fraction per jet $(1 + \text{had/em})^{-1}$ of calorimeter deposition, an upper bound of 1.25 on the missing energy ratio $R(H_T^{\text{miss}})$ of hard ($p_T \geq 50$ GeV) to soft ($p_T \geq 30$ GeV) jets, and upper bounds of 10 GeV and 25 GeV, respectively, for the transverse momentum of isolated light leptons (electron, muon) and photons. The latest CMS report more specifically describes $R(H_T^{\text{miss}})$ as the ratio of missing energy computed from only hard jets to the same as computed from the calorimeter tower estimate, but the intended function as a blockade against substantial cumulative failures of per jet limit on transverse momentum is identical, and we expect comparable outcomes. As a safeguard, we also secondarily filter with regards to the missing energy reported natively by PGS4. The “biased” $\Delta\phi^*$ statistic, designed to help distinguish actual missing energy signals from detector mismeasurements, remains disabled. The CMS collaboration does employ $\Delta\phi^*$ in conjunction with filters on proximity of the likely source of missing energy to masked regions of the electromagnetic calorimeter. We do not attempt to replicate either this behavior or a similar treatment of the CMS barrel-endcap gap. For our immediate comparison with Section (2.1) of the CMS source document [1], the minimal jet count of three is temporarily suspended, with two-jet events also allowed. A lower bound of 0.55 is generally imposed on α_T , which was like $\Delta\phi^*$, also devised to help isolate legitimate missing transverse energy, although this cut is also sometimes also relaxed, either for the sake of comparison or for direct histogram binning

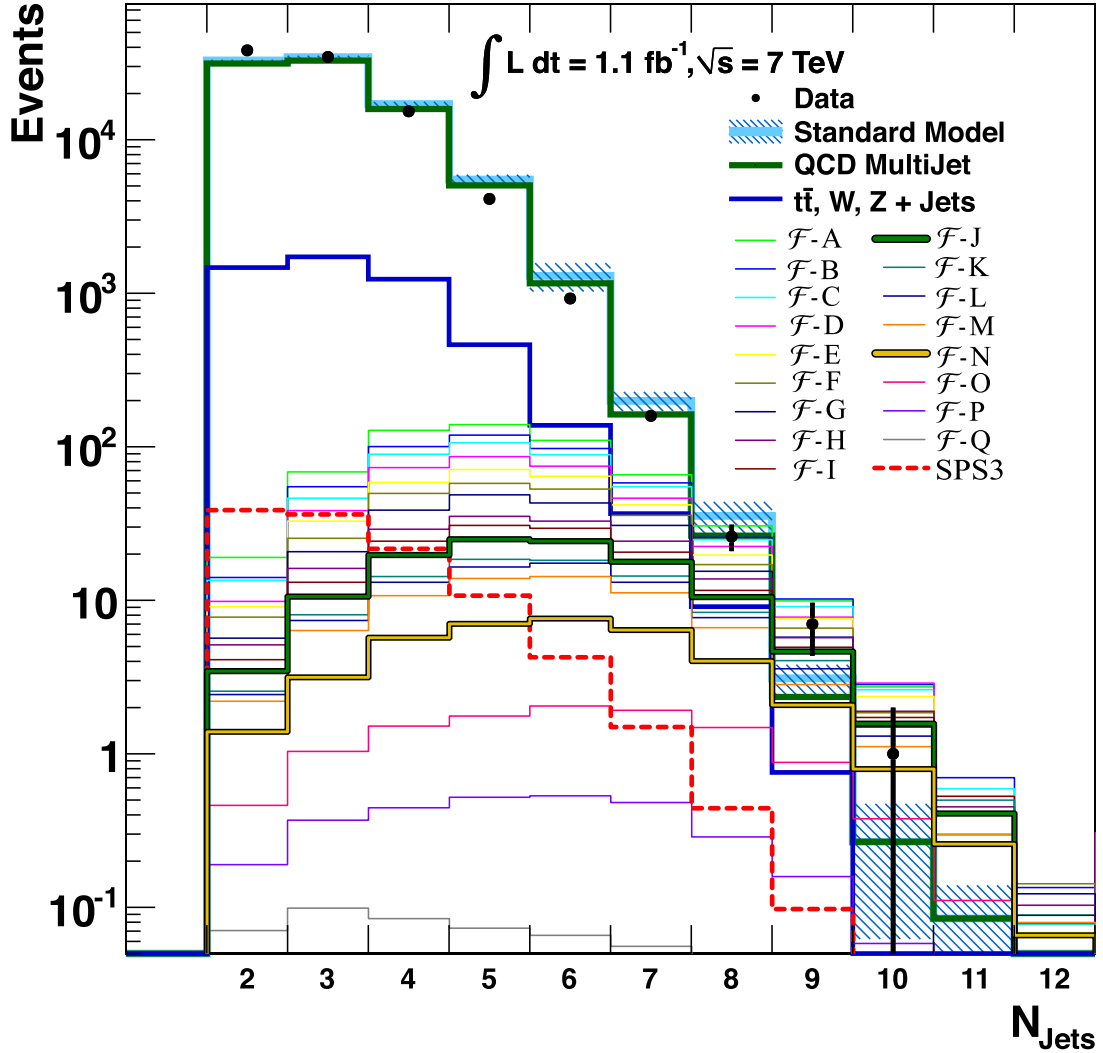


FIG. 1: The CMS Preliminary 2011 signal and background statistics for 1.1 fb^{-1} of integrated luminosity at $\sqrt{s} = 7 \text{ TeV}$, as presented in [1], are reprinted with an overlay consisting of a Monte Carlo collider-detector simulation of the No-Scale \mathcal{F} - $SU(5)$ model space benchmarks of Table (I), and the CMSSM benchmark SPS3. An experimentally favored region consistent with the bare-minimal experimental constraints of [9] and both the $(b \rightarrow s\gamma)$ process and contributions to the muon anomalous magnetic moment $(g-2)_\mu$ within the \mathcal{F} - $SU(5)$ model space is represented by the emphasized gold contour. The emphasized green contour indicates the estimated lower bound on the parameter space after application of the CMS 1.1 fb^{-1} analysis. The plot counts events per jet multiplicity, with no cut on α_T .

against α_T itself. The role of the α_T cut in ultra-high jet multiplicity searches is of particular interest to our group, and we shall revisit the topic in detail in Section (VI).

In the figures described in this section, we reprint the signal and CMS Preliminary SM background statistics presented in Ref. [1], overlaying our Monte Carlo simulation of each No-Scale \mathcal{F} - $SU(5)$ benchmark [10–12], as well as the CMSSM benchmark “Snowmass Points and Slopes” SPS3 [56]. Consult Table (I), which is printed following in Section (V), for the map between the alphabetical model index and the corresponding LSP, gaugino, and vector-like masses m_{LSP} , $M_{1/2}$ and M_V . Our simulation was performed using the **MadGraph** [57, 58] suite, including the standard **MadEvent** [59], **PYTHIA** [60]

and **PGS4** [61] chain, with post-processing performed by a custom script **CutLHCO** [62] (available for download) which implements the desired cuts, and counts and compiles the associated net statistics. All 2-body SUSY processes have been included in our simulation, which follows in all regards the procedure detailed in Ref. [8]. Our SUSY particle mass calculations have been performed using **MicrOMEGAs 2.1** [63], employing a proprietary modification of the **SuSpect 2.34** [64] codebase to run the RGEs. Most often, we oversample the Monte Carlo and scale down to the required luminosity, which can have the effect of suppressing statistical fluctuations.

Figure (1) depicts the event count per jet multiplicity, as based on Figure (1a) from Section (2.1) of Ref. [1]. It

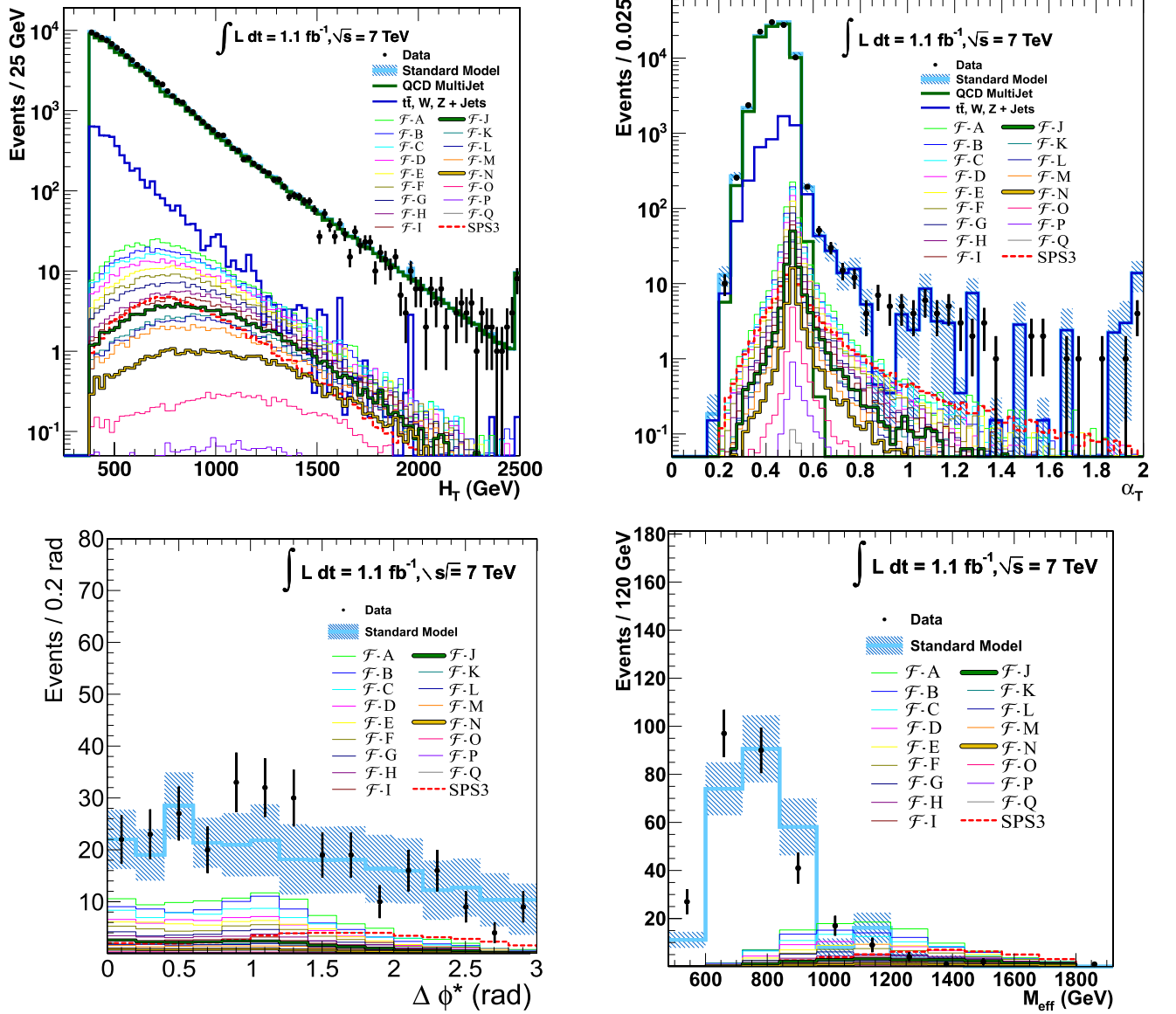


FIG. 2: The CMS Preliminary 2011 signal and background statistics for 1.1 fb^{-1} of integrated luminosity at $\sqrt{s} = 7 \text{ TeV}$, as presented in [1], are reprinted with an overlay consisting of a Monte Carlo collider-detector simulation of the No-Scale \mathcal{F} - $SU(5)$ model space benchmarks of Table (I), and the CMSSM benchmark SPS3. An experimentally favored region consistent with the bare-minimal experimental constraints of [9] and both the $(b \rightarrow s\gamma)$ process and contributions to the muon anomalous magnetic moment $(g-2)_\mu$ within the \mathcal{F} - $SU(5)$ model space is represented by the emphasized gold contour. The emphasized green contour indicates the estimated lower bound on the parameter space after application of the CMS 1.1 fb^{-1} analysis. Histograms are displayed for the four statistics H_T , α_T , $\Delta\phi^*$, and M_{eff} . The lower two plots feature a cut on $\alpha_T \geq 0.55$, while this is suppressed in the upper two plots.

is most important to note that the α_T cuts have been bypassed in this plot. The logarithmic event scaling generally allows one to disregard component signals which exhibit substantial visual separation below the leading term. The SM expectation is, for the most part, a very good fit to the data in this plot, although there is an intriguing excess observed above the SM background in the nine jet bin. Visually, the central value of this excess appears to be about four events, and allowing for extremities in the variation of both the expectation and the ob-

servation, it seems that a range of one to seven events might be considered marginally consistent. It seems in particular that the lighter portion of the No-Scale \mathcal{F} - $SU(5)$ model space, as represented by the lower alphabetically assigned indices (A-E), might be considered to overproduce above the observation. Above this extreme, there is a healthy swath of parameter space that seems quite nicely capable of accounting for the observation, carrying labels (F) and greater. We have given graphical emphasis to two points, \mathcal{F} -J (bold green) and \mathcal{F} -N (bold

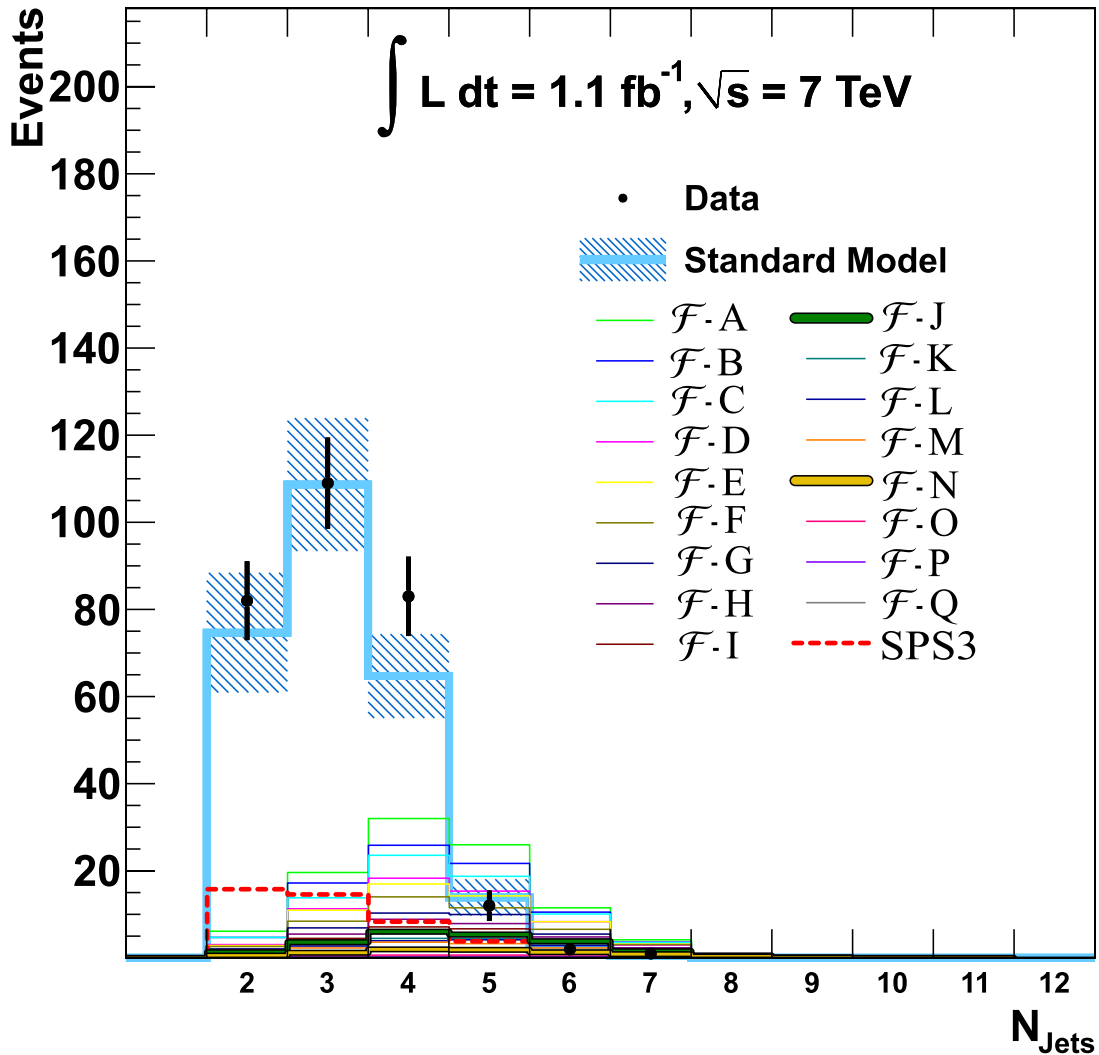


FIG. 3: The CMS Preliminary 2011 signal and background statistics for 1.1 fb^{-1} of integrated luminosity at $\sqrt{s} = 7 \text{ TeV}$, as presented in [1], are reprinted with an overlay consisting of a Monte Carlo collider-detector simulation of the No-Scale $\mathcal{F}\text{-}SU(5)$ model space benchmarks of Table (I), and the CMSSM benchmark SPS3. An experimentally favored region consistent with the bare-minimal experimental constraints of [9] and both the $(b \rightarrow s\gamma)$ process and contributions to the muon anomalous magnetic moment $(g - 2)_\mu$ within the $\mathcal{F}\text{-}SU(5)$ model space is represented by the emphasized gold contour. The emphasized green contour indicates the estimated lower bound on the parameter space after application of the CMS 1.1 fb^{-1} analysis. The plot counts events per jet multiplicity, with a cut on $\alpha_T \geq 0.55$.

gold), with the green defining the estimated boundary of our surviving space subsequent to the present analysis, and the gold representing the most experimentally favored region consistent with the bare-minimal experimental constraints of [9] and both the $(b \rightarrow s\gamma)$ process and contributions to the muon anomalous magnetic moment $(g - 2)_\mu$. We note also that the CMSSM representative SPS3, shown in bold red dash, dramatically underperforms observations. A similar result was clear in the source document with regards to two tested CMSSM representatives, the benchmark models LM4 and LM6, with LM6 most similar to our SPS3 and faring the worse. We can already see in this figure a considerably more rapid fatiguing of the SM and CMSSM signals with increas-

ing jet count than is experienced by any of the No-Scale $\mathcal{F}\text{-}SU(5)$ candidates. The eight and ten jet bins seem to consistently disfavor a similar swath of light models, although there is again no constraint on the heavier models. There were apparently no CMS observations in the eleven and twelve jet bins. Since our favored expectations are less than one event in each of these regions, we do not consider the statistics to be cautionary.

Figure set (2) makes a similar treatment of Figures (1a,1c,2a and 2b) of Ref. [1]. The α_T cut is disabled in the upper two plots, but active in the lower. Whereas the No-Scale $\mathcal{F}\text{-}SU(5)$ histograms merge into something of a continuum, one is less visually interested in tracking the behavior of single model elements than

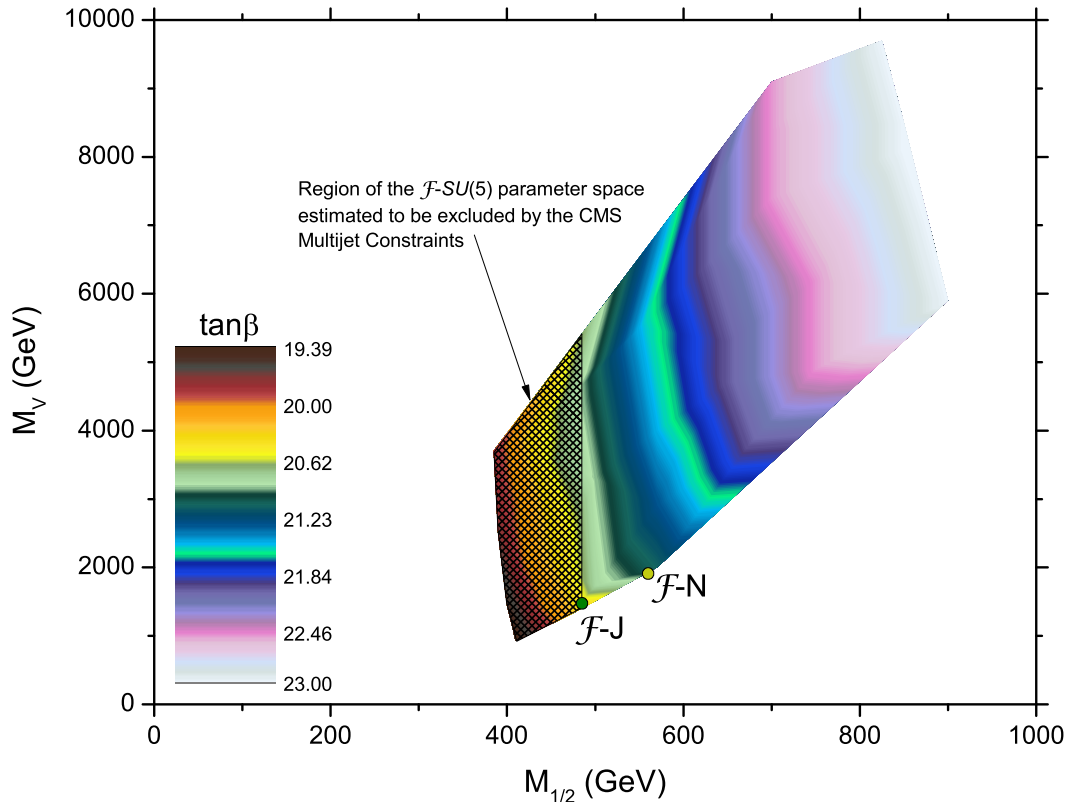


FIG. 4: The bare-minimally constrained parameter space of No-Scale \mathcal{F} - $SU(5)$ is depicted as a function of the gaugino boundary mass $M_{1/2}$, the vector-like mass M_V , and via the color key, the ratio of Higgs VEVs $\tan\beta$. The region estimated to be disfavored by the first inverse femtobarn of integrated LHC luminosity has been marked with crosshatch. An experimentally favored region consistent with the bare-minimal experimental constraints of [9] and both the $(b \rightarrow s\gamma)$ process and contributions to the muon anomalous magnetic moment $(g - 2)_\mu$ within the \mathcal{F} - $SU(5)$ model space is represented by the gold point. The green point is a representative benchmark that indicates the estimated lower bound on the parameter space after application of the CMS 1.1 fb^{-1} analysis.

delineation of the model space boundary. We observe no constraint from either of the upper figures. The histogram in α_T , however, does effectively demonstrate the rather more rapid falloff of the No-Scale \mathcal{F} - $SU(5)$ models with respect to larger values of this statistic. Again, the SPS3 benchmark seems to behave most similarly to the externally studied LM6 example.

The source documents of the lower two figures opt for a linear scaling which imposes some visual compression on the model space. In the $\Delta\phi^*$ histogram at lower left, we observe relatively low tension relative against any of the presented models. The most interesting feature of this plot is in the angular range of 0.8 to 1.4 radians, where the uncertainty of the observed signal remains in reasonable proximity to the background, though one could envision a possible excess above the Standard Model. Curiously, certain of the lighter models seem well suited to explaining an excess, perhaps at the cost of reducing somewhat the observed parity with the SM signal from 0.0 to 0.8 radians. Our lighter bold-printed model, \mathcal{F} -J, produces about two events in this region, which is acceptable. There are a few bins, namely at 0.7, 1.9 and 2.7

radians, where the lightest \mathcal{F} - $SU(5)$ models, and/or the SPS3 benchmark might be said to exceed the measurement, although each of these data points also defy the trend established by their neighbors. Likewise, the LM4 model considered in the source document appears in some cases to overproduce. We also mention the fact that the CMSSM models SPS3 (and similarly again LM6) feature a flatter angular distribution in $\Delta\phi^*$ than their \mathcal{F} - $SU(5)$ counterparts, which tend to peak earlier, at about one radian, and then fall off faster; we will return to this point in Section (VI).

The lower right-hand element of Figure Set (2) is a histogram in the “effective mass” M_{eff} of the event, which we take to be a scalar sum of all measured transverse energy and missing transverse energy, for all event beam fragments, including soft hadronic jets, leptons and photons. One initial feature to catch the eye is a possible excess at around 1 TeV. It seems that a post-SM production in the wide range of about 1 to 15 events is minimally consistent. Only the very lightest \mathcal{F} - $SU(5)$ models seem to suffer here. Again, models in the vicinity of \mathcal{F} -J perform favorably. Curiously, the externally studied bench-

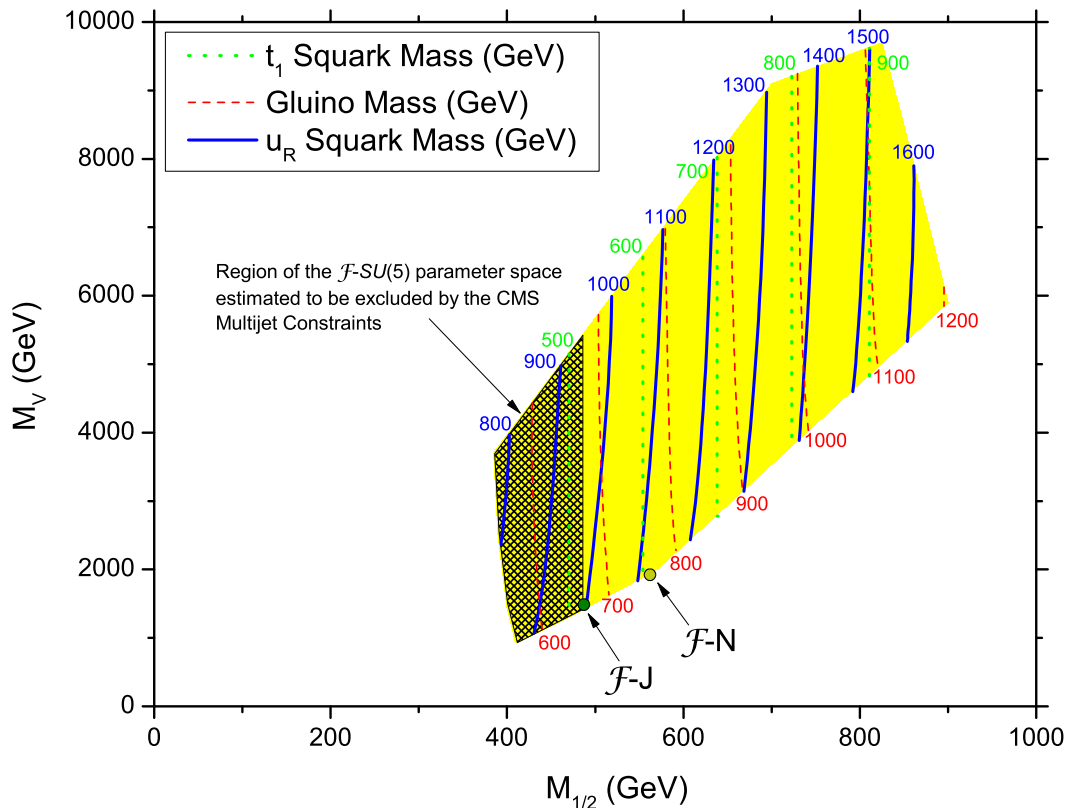


FIG. 5: The bare-minimally constrained parameter space of No-Scale \mathcal{F} - $SU(5)$ is depicted as a function of the gaugino boundary mass $M_{1/2}$, the vector-like mass M_V , and via the solid, dashed, and dotted contour lines, the masses in GeV of the light stop squark \tilde{t}_1 , gluino \tilde{g} , and right-handed up squark \tilde{u}_R . The upper bound on the region estimated to be disfavored by the first inverse femtobarn of integrated LHC luminosity has been marked with the crosshatched pattern. An experimentally favored region consistent with the bare-minimal experimental constraints of [9] and both the $(b \rightarrow s\gamma)$ process and contributions to the muon anomalous magnetic moment $(g-2)_\mu$ within the \mathcal{F} - $SU(5)$ model space is represented by the gold point. The green point is a representative benchmark that indicates the estimated lower bound on the parameter space after application of the CMS 1.1 fb^{-1} analysis. The lower bound on $m_{\tilde{g}}$ for the entire model space occurs in the range of 658-674 GeV, while the lower bound on $m_{\tilde{u}_R}$ transpires in the span of 956-1000 GeV. The lower bound for all the heavy squarks ($m_{\tilde{t}_2}, m_{\tilde{b}_R}, m_{\tilde{b}_L}, m_{\tilde{u}_R}, m_{\tilde{u}_L}, m_{\tilde{d}_R}, m_{\tilde{d}_L}$) occurs in the range of 854-1088 GeV. The minimum boundary on $m_{\tilde{t}_1}$ is about 520 GeV.

mark LM4 dramatically overproduces, not only here, but also for larger values of M_{eff} , approaching 2 TeV. Likewise, several of the previously disfavored lighter \mathcal{F} - $SU(5)$ benchmarks, and to some degree also SPS3, overproduce in the range of about 1.1 TeV to 1.8 TeV. We see no model under consideration which can account for the observed excess in the 480-720 GeV region, which might be taken to engender some skepticism of the measurements or SM modeling in this region.

We turn attention now to Figure (3), adapted from Figure (2c) of Ref. [1], which is a second plotting of measured events by jet count, but now with the α_T cut firmly in place. In the source document, model LM4 again dramatically overproduces across the range, and is strongly disfavored. We see no strong tension between any of the models presently considered in this work, for jet counts of 2, 3, or 4. At five jets, it seems that the post-SM contribution should not exceed five or six events. This cuts rather hard against the No-Scale \mathcal{F} - $SU(5)$ model

space, but in a manner similar to what has been already observed. Benchmark \mathcal{F} -J sits near the edge of the permissible value, and the heavier bold-printed benchmark, \mathcal{F} -N performs quite well. Although it is difficult to see in this figure, the SM tracks the observation closely here for six or more jets, with low uncertainties indicated, and it seems that any substantial extraneous production should be disfavored. In this regard, at a count of six jets, the \mathcal{F} -J benchmark does experience some strain, although the heavier models around \mathcal{F} -N are quite comfortable. Our simulation of the CMSSM point SPS3 avoids conflict throughout this metric, again tracking nicely with the published LM6 model. We remark, not inadvertently, that Figure (3), as compared to Figure (1) seems to favor models in which high jet events are heavily suppressed by the α_T statistic.

In Figure (4), we display the full bare minimally constrained [9] parameter space of No-Scale \mathcal{F} - $SU(5)$, including application of a crosshatch over the lighter spec-

tra which we would estimate to be excluded by the analysis of this section. Although a large number of our originally selected benchmarks were placed within this lighter region, as a relative portion of the full hyper-volume, the model reduction is surprisingly minor. The vertically established exclusion boundary, which is appropriate inasmuch as the sparticle spectrum is virtually independent of $\tan\beta$ and the top quark m_t or the vector-like M_V masses, emphasizes the reductionism of parameterization which is inherent in No-Scale \mathcal{F} - $SU(5)$. The SPS3 benchmark, which has been our standard control sample in recent work, was chosen in some part for its viability in the face of earlier generation search results. This accounts, of course, for its comparably heavy LSP mass. The crystal clear exclusion of this model, and likewise of CMSSM representatives in its not-so-immediate vicinity, therefore speaks quite strongly to the current trouble which the mSUGRA/CMSSM framework is experiencing.

The analysis of Ref. [1] concluded that squark and gluino masses of 1.25 TeV may now be excluded for values of the unified scalar mass at the GUT scale of $m_0 < 530$ GeV. However, as depicted by the light stop squark, gluino, and right-handed up squark mass contours in Figure (5), the No-Scale \mathcal{F} - $SU(5)$ model space does not share a similar fate. Our estimated lower bound on the single \mathcal{F} - $SU(5)$ model parameter $M_{1/2}$ of 485 GeV translates into a lower bound on the gluino mass of 658-674 GeV for the entire model space, notably below the gluino mass constraint of 1.25 TeV established for the CMSSM for $m_0 < 530$ GeV. In a similar vein, we choose the right-handed up squark \tilde{u}_R to graphically represent all the heavy squarks, and we likewise discover that the lower bound on $m_{\tilde{u}_R}$ to be 956-1000 GeV, also substantially below the CMSSM squark mass constraint of 1.25 TeV for $m_0 < 530$ GeV. When considering all the heavy squarks ($m_{\tilde{t}_2}, m_{\tilde{b}_R}, m_{\tilde{b}_L}, m_{\tilde{u}_R}, m_{\tilde{u}_L}, m_{\tilde{d}_R}, m_{\tilde{d}_L}$), the lower mass constraints in the \mathcal{F} - $SU(5)$ model space lie within 854-1088 GeV. It is important to note again that the light stop \tilde{t}_1 mass is less than the gluino mass in \mathcal{F} - $SU(5)$, apparent through the unique mass hierarchy $m_{\tilde{t}} < m_{\tilde{g}} < m_{\tilde{q}}$, thus the light stop mass limit will also be much less than that of the CMSSM, with an \mathcal{F} - $SU(5)$ light stop minimum mass of about 520 GeV.

IV. ULTRA-HIGH JET MULTIPLICITIES

The ultra-high jet signal of No-Scale \mathcal{F} - $SU(5)$ was first discussed in Refs. [7, 8], and is based upon the stable sparticle hierarchy $m_{\tilde{t}} < m_{\tilde{g}} < m_{\tilde{q}}$ of a light stop and gluino, much lighter than all other squarks, which exists across the full model space. This mass hierarchy is expected to strongly generate back-to-back pair production events, *e.g.* of two heavy squarks $\tilde{q}\tilde{\bar{q}}$, which proceed by a decay such as $\tilde{q} \rightarrow q\tilde{q}$, followed by (where we identify the virtual tops with parentheses) $\tilde{g} \rightarrow \tilde{t}_1(\tilde{t}) \rightarrow t\tilde{t}\tilde{\chi}_1^0 \rightarrow W^+W^-b\tilde{b}\tilde{\chi}_1^0$ or $\tilde{g} \rightarrow \tilde{t}_1(\tilde{t}) \rightarrow b\tilde{t}\tilde{\chi}_1^+ \rightarrow W^-b\tilde{b}\tilde{\tau}_1^+\nu_\tau \rightarrow W^-b\tilde{b}\tau^+\nu_\tau\tilde{\chi}_1^0$ (plus conjugate

processes), which produces up to eight primary jets, considering only the initial hard scattering cascade. This count may be substantially increased by the further cascaded fragmentation and hadronization into final state showers of photons, leptons, and mixed jets.

We have proposed a specific alternative to the leading “CMS” style intermediate jet count (3,4,5) SUSY searches which is retuned for the emphasis of high and ultra-high (9,10,11,12,...) jet content signals. The details of the proposed cutting strategy, which we will refer to by the “ULTRA” shorthand, are given in Section (IV) of Ref. [8]. Although various optimizations in the limiting jet count and transverse momentum p_T per jet were considered for the ULTRA cuts in the cited work, we settled there on, and maintain here, the aggressive combination of ($p_T > 20$, jets ≥ 9) as the baseline indicator of this selection procedure. The simultaneous reduction of the p_T jet threshold from 50 relative to the CMS style cuts is an essential parallel ingredient in the prescription for revealing an enhanced quantity of softer jets. We do, however, maintain demands that the two leading jets carry 100 GeV of transverse momentum each. Pseudorapidity cuts of $\eta \leq 3$ for all jets, and of $\eta \leq 2$ for the leading jet, are likewise enforced. Since the ultra-high jet regime is greatly suppressed in the SM backgrounds, we have been able to relax certain of the harsh cuts which are very effective for separating out the MSSM in intermediate jet searches, but which simultaneously exert a costly attrition against the No-Scale \mathcal{F} - $SU(5)$ signal. Specifically, we effectively disable the cuts on the electromagnetic fraction per jet, α_T and the missing energy ratio $R(H_T^{\text{miss}})$. These distinctions are critical, as we shall elaborate in Section (VI), to the success of ultra-high jet multiplicity search strategies. We emphasize again though, validating the old adage that less is sometimes more, that the ultra-high jet blockade itself forms a sufficiently strong discriminant against both the SM and typical mSUGRA/CMSSM attempts at a post-SM solution. A cautious reconsideration of lower order SM background contributions will be the topic of Section (VIII).

In more recent work [11, 12], we have undertaken a massive Monte Carlo simulation of the collider-detector response of the the full bare-minimally constrained [9] parameter space of No-Scale \mathcal{F} - $SU(5)$, modeling both the present LHC center of mass energy $\sqrt{s} = 7$ TeV and upgrades which extend into the bright future of a $\sqrt{s} = 14$ TeV beam. In addition to a prediction for the absolute detection prospects of a given model under certain conditions, there are two sensible modes of comparison which one may consider: A) it is possible to contrast competing models, taking for example respective elements from the viable CMSSM and \mathcal{F} - $SU(5)$ parameter spaces, while keeping the detector cut methodology constant; B) one may highlight enhancements in the visibility of a single model which are attributable to changes in the search methodology, and in particular to the data selection cuts which are employed. Both comparative modes have the advantage over an absolute study that

particular uncertainties may be expected to cancel between the respective analyses. We have considered both modes A and B in the past, and will revisit both again here, although our primary interest will be with regards to mode B, for the reasons described following.

Immediately, our interest has been greatly piqued by the announcements made during the recent conference season that various analyses of LHC data in the high jet multiplicity (6, 7, 8, ...) channels are currently underway. Specifically, the ATLAS collaboration stated that they have amassed 1.23 fb^{-1} , and presented analyses of up to 1.0 fb^{-1} for the mono-jet and di-jet channels with no evidence of new physics. Results for searches targeted at exotic models, in five or more jets with a per jet transverse momentum threshold of $p_T \geq 50 \text{ GeV}$, remain pending. In Ref. [65], the ATLAS collaboration looked at multi-jet searches up to 6 jets, applying a very hard Cut of $p_T \geq 60 \text{ GeV}$, although the data sampling was only 2.4 pb^{-1} .

The CMS collaboration meanwhile presented new data at the level of 1.1 fb^{-1} for mono and di-jet searches, but reverted to the prior level of 35 pb^{-1} for the study of events with ≥ 6 jets from pair-produced gluinos. While the stated target of CMS searches into this high jet territory [66] is the search for exotic R-parity violating SUSY models and Technicolor, any basic experimental physics results are of course model-independent, and we still take notice. A most interesting physics analysis summary [1] has also been released by the CMS collaboration, focusing on application of the α_T variable, but in some places distributing events binned by integral jet count from 2 up to 12; this is the report which formed the centerpiece of our discussion in Section (III).

A key aim of the next section will then be distinguishing among various high and ultra-high jet cutting scenarios, attempting to quasi-continuously span the range of possibilities, demonstrating firstly that not all such high-jet selection cuts are created equal, and secondly outlining precisely what material differences in outcome might be expected within the No-Scale $\mathcal{F}\text{-}SU(5)$ model space by the application of the various cuts considered. We will continue to replicate all simulation and analysis in the context of our CMSSM control sample, the “Snowmass Points and Slopes” benchmark SPS3 [56]. To a certain extent, it might appear that we already have at least a portion of what we are asking for, inasmuch as the data for distribution of event count per jet has been released, and one may simply truncate the counts below any certain desired high jet threshold. Indeed, we have in the prior section demonstrated that the surviving No-Scale $\mathcal{F}\text{-}SU(5)$ model space may very effectively, and even precisely, account for certain anomalies observed in the presented data. However, we suggest in particular that the additional filtering criteria imposed under the global CMS style cutting procedure has potentially decimated the ultra-high (9, 10, 11, 12, ...) jet multiplicity content, and that a much stronger validation might thus be immediately possible.. This is a critical point on which

we shall immediately begin to elaborate.

V. THE TEN-FOLD WAY

In Ref. [11], we introduced a discovery index N , given by the following expression, where S and B are respectively the observed signal and background at some reference luminosity, conveniently chosen as 1 fb^{-1} .

$$N = \frac{12.5 B}{S^2} \times \left[1 + \sqrt{1 + \left(\frac{2S}{5B} \right)^2} \right] \quad (1)$$

The value of N is the relative luminosity factor by which both S and B should be scaled in order to achieve a baseline value of five for the statistic of merit $S/\sqrt{B+1}$ for overall model visibility. Note that in the limit of large backgrounds, where the “+1” safety factor is unnecessary, the discovery index reduces to $N = 25B/S^2$. In that work, our interest was the absolute likelihood of discovery of various elements of the bare minimally constrained [9] model space of No-Scale $\mathcal{F}\text{-}SU(5)$. Correspondingly, we published there in Table (1) a detailed tabulation of the $S/\sqrt{B+1}$ statistic, at $\sqrt{s} = 7 \text{ TeV}$ and 1 fb^{-1} of luminosity, for each selected benchmark representative of the model space, as well as the CMSSM control sample SPS3 [56]. We found a wide range of possible values for N , ranging from 0.05 to 38.9 for LSP masses ranging respectively from about 75 to 190 GeV. This was supplemented by Figure (1) of the same work, wherein we showed event count histograms in the missing transverse energy H_T^{miss} for all models, for beam energies of $\sqrt{s} = (7, 8, 10, 12 \text{ and } 14) \text{ TeV}$, and by Figure (2), wherein we plotted the discovery index N for each of the same. The discovery index was found to increase exponentially with the LSP mass, and also to depend sharply on the beam energy, decreasing by a factor between about 50 and 3500 under a doubling of the beam energy from 7 to 14 TeV, for the lightest and heaviest spectra respectively. In conjunction with the sister publication [12], wherein specific mass limits were projected for key SUSY partners under various collider conditions, we concluded that the model space of No-Scale $\mathcal{F}\text{-}SU(5)$ would begin to be effectively probed under the current operating environment of 1 fb^{-1} at $\sqrt{s} = 7 \text{ TeV}$, with a majority of the remainder accessible to an identical sampling of 1 fb^{-1} after the $\sqrt{s} = 14 \text{ TeV}$ upgrade, and the entirety within reach of 10 fb^{-1} of high energy data. Of course, as we indicated at the time, these results were entirely dependent upon adoption of the optimized Ultra-high jet cuts.

The purpose of the current section is a comparative study between various cut strategies, which attempt to span the continuum between the canonical “CMS” style ≥ 3 jet cuts which we modeled in Ref. [8], and the optimized ≥ 9 ultra-high jet multiplicity strategy, again spanning present and future collider energies, and the complete bare minimally constrained $\mathcal{F}\text{-}SU(5)$ model space,

as well as our standard CMSSM control sample. We have chosen four representative cutting scenarios, including the two previously studied, *i.e.*, the baseline CMS style ≥ 3 jet scenario with updates as described in Section (III), which we will here dub “CMS:3”, and the baseline ultra-high ≥ 9 jet scenario, which will be referred to as “ULTRA:9”. To this set, we add two additional methodologies, which represent each a change only in the jet count threshold, being similar to their source procedures in all other regards. From the CMS:3 cuts, we clone the new “CMS:6” selector, raising the jet threshold from 3 to 6, and likewise lowering the threshold from 9 to 6 jets in the original ultra-high procedure, we introduce the new “ULTRA:6” selector.

It should be noted that in our absolute studies of ultra-high jet cutting scenarios up to this point, we have argued that the $t\bar{t}$ +jets background should constitute the leading SM competition, being in fact alone sufficient to model the full standard model (SM) process contribution. In the present work, where we must consider also selection cuts which do not make heavy use of the net jet count to significantly reduce the SM backgrounds, we should certainly cast a wider net. In particular, for ≥ 6 jet searches, it would seem prudent at least to also consider the W^\pm processes. For three or more jets, it seems that the gates are cast essentially wide open. There is an interesting reference available [67] which provides rather comprehensive background modeling statistics for the full set of SM components up to six jets, but these are before the application of any cuts, which makes a direct translation into our present numerical calculations rather difficult. However, since the interest is again now purely comparative, one may naïvely suspect that the common divisor of a roughly proportional background rescaling will cancel to a good approximation, and that reuse of the simplified Monte Carlo samples is valid.

This is in fact not strictly correct, as various components of the background will react in an individually differentiated manner to the jet threshold cut parameter. We will nevertheless proceed as if this approximation is correct for the interim, following up in Sections (VII and VIII) with an attempt to provide reasonable estimates, based upon the most recently presented LHC background measurements [1], of how the inclusion of a more realistic SM modeling might affect the absolute detection prospects of No-Scale \mathcal{F} - $SU(5)$, especially under lower jet multiplicity selection thresholds. Immediately, one may anticipate that if the unmodeled backgrounds, including vector boson production, possibly also associated with top quark or jet production, pure QCD (2, 3, 4) multijet events, and all $b\bar{b}$ associated processes, are indeed unable to substantially penetrate the ultra-high jet multiplicity barrier, the differential visibility of No-Scale \mathcal{F} - $SU(5)$ in the ULTRA cuts relative to the CMS cuts will improve. Indeed, we mention preemptively that these considerations could potentially escalate the advertised by an additional factor in the range of about five to ten.

We present in Table (I), for each single model taken in

turn, the ratio representing the discovery index N which applies under one of three competing selection cut scenarios, divided by the value of N which is achieved in our baseline ultra-high jet paradigm. The incredibly strong dependence of the discovery index on the LSP mass and on the collider energy which was described previously is found to be substantially tamed by the chosen ratio. The residual distinctions between various model elements are found to be stronger, on balance, than the distinctions arising from escalation of the beam energy. We therefore average over the latter in the primary table. In Table (II), we do explicitly demonstrate the energy dependence by averaging instead over the model, although a wholly systematic effect is not readily apparent.

We can see clearly from Table (I) that the traditionally styled CMS:3 cuts are actually quite appropriate for elucidating the signal of the CMSSM, in fact some factor of order 10 more appropriate than the most severe ULTRA variety of cuts. Conversely, the ULTRA:9 cuts are definitively the best tested cut for application to the No-Scale \mathcal{F} - $SU(5)$ models, and likewise some factor of order 10 superior to the CMS:3 variety, for this purpose. However, this analysis, by design is purely comparative, and reveals nothing about the absolute visibility of either model. For this purpose, we must either directly access the discovery index N , accepting also the associated complication of the SM background, or compose again an appropriate ratio. We will opt to evaluate the ratio of the discovery index N for the No-Scale \mathcal{F} - $SU(5)$ models divided by the CMSSM discovery index. The backgrounds literally cancel in this case, at least in the large background limit, and the result reduces essentially to a ratio of inverse signals-squared. It is difficult, though, to establish a rationale for which points of the respective model spaces are to be compared, as the expected signal varies dramatically with the LSP mass. Purely as a matter of individual discretion, we will partition the No-Scale \mathcal{F} - $SU(5)$ benchmarks into light ($m_{\text{LSP}} < 95$ GeV), medium ($95 \text{ GeV} \leq m_{\text{LSP}} < 135$ GeV), and heavy ($135 \text{ GeV} \leq m_{\text{LSP}}$) groups, and give ratios in Table (III) for the CMSSM benchmark SPS3 discovery index in comparison to the average \mathcal{F} - $SU(5)$ discovery index, for each mass grouping, and for each beam energy.

In absolute terms, Table (III) demonstrates that the lighter elements of No-Scale \mathcal{F} - $SU(5)$ are generally about equally as visible as the SPS3 benchmark, under the CMS:3 cutting scenario. This highlights the fact established in Section (III) that these lighter models, along with huge swaths of the mSUGRA/CMSSM structure, have effectively been disallowed by the first inverse femtobarn of LHC data. The ULTRA:9 cuts are again about ten times better for \mathcal{F} - $SU(5)$, and about ten times worse for the CMSSM representative, but we can now see that both differentials work in the same direction. In other words, while the CMS cuts are indeed very bad for No-Scale \mathcal{F} - $SU(5)$, the lighter elements ($m_{\text{LSP}} \leq 95$ GeV) of this model can still compete for visibility in standard searches when put up against sufficiently compa-

TABLE I: Seventeen representative points, labeled \mathcal{F} -(A...Q), are selected for display from the No-Scale \mathcal{F} - $SU(5)$ model space, satisfying the bare-minimal phenomenological constraints outlined in Ref. [9]. In addition, a CMSSM control sample is supplied, corresponding to the “Snowmass Points and Slopes” benchmark SPS3 [56]. For this latter point, the M_V column is appropriated instead for M_0 . Units of GeV are taken for the dimensionful parameters $m_{\text{LSP}}, M_{1/2}, M_V, m_t$ and M_0 . The rightmost three columns display the ratio of the discovery index N for the given model, under two different cutting methodologies. The constant reference denominator is the Ultra-high multiplicity selection cut on at least 9 jets (ULTRA:9). This is compared to the traditional CMS style cuts with at least 3 (CMS:3) or 6 (CMS:6) jets, as well as a replica of the Ultra-high style cut with the jet threshold reduced to 6 (ULTRA:6), all else being equal. The results are averaged over center-of-mass collision energies of $\sqrt{s} = 7, 8, 10, 12$ and 14 TeV.

Model	m_{LSP}	$M_{1/2}$	M_V	$\tan \beta$	m_t	$\frac{N(\text{CMS:3})}{N(\text{ULTRA:9})}$	$\frac{N(\text{CMS:6})}{N(\text{ULTRA:9})}$	$\frac{N(\text{ULTRA:6})}{N(\text{ULTRA:9})}$
\mathcal{F} -A	74.8	385	3575	19.8	172.5	3.3	9.4	0.6
\mathcal{F} -B	75.0	395	2075	19.7	172.5	3.7	9.4	0.7
\mathcal{F} -C	74.7	400	1450	19.5	173.7	4.1	10.0	0.7
\mathcal{F} -D	75.0	410	925	19.4	174.4	4.8	10.4	0.8
\mathcal{F} -E	83.2	425	3550	20.4	172.2	4.6	8.5	0.9
\mathcal{F} -F	83.1	435	2000	20.1	173.1	5.8	9.1	1.0
\mathcal{F} -G	82.8	445	1125	19.9	174.4	6.8	10.0	1.1
\mathcal{F} -H	92.2	465	3850	20.7	172.2	7.5	8.3	1.3
\mathcal{F} -I	92.2	475	2400	20.6	173.1	8.6	8.7	1.4
\mathcal{F} -J	92.1	485	1475	20.4	174.3	9.8	9.2	1.6
\mathcal{F} -K	100.5	505	3700	21.0	172.6	10.4	7.6	1.9
\mathcal{F} -L	100.2	510	2875	21.0	174.1	11.4	8.0	2.0
\mathcal{F} -M	100.0	520	1725	20.7	174.4	12.0	8.0	2.1
\mathcal{F} -N	108.8	560	1875	21.0	174.4	15.7	7.1	2.7
\mathcal{F} -O	133.2	650	4700	22.0	173.4	20.7	5.8	4.1
\mathcal{F} -P	155.9	750	5300	22.5	174.4	10.3	2.2	4.3
\mathcal{F} -Q	190.5	900	6000	23.0	174.4	7.5	1.7	4.3
\mathcal{F} -Average	100.8	513	2859	20.7	173.5	8.7	7.9	1.8
SPS3	161.7	400	$M_0 = 90$	10.0	175.0	0.11	0.72	0.26

TABLE II: Discovery index ratios are presented in a fashion similar to Table (I), but averaged over the model space, and displayed independently per each collider energy.

Model	\sqrt{s}	$\frac{N(\text{CMS:3})}{N(\text{ULTRA:9})}$	$\frac{N(\text{CMS:6})}{N(\text{ULTRA:9})}$	$\frac{N(\text{ULTRA:6})}{N(\text{ULTRA:9})}$
\mathcal{F} - $SU(5)$	7	7.9	8.1	1.9
	8	9.9	9.7	2.1
	10	9.5	6.5	2.0
	12	8.2	6.7	1.7
	14	7.9	8.2	1.5
SPS3	7	0.04	0.57	0.16
	8	0.08	1.02	0.21
	10	0.13	0.50	0.32
	12	0.14	0.62	0.30
	14	0.19	0.87	0.30

rably heavier elements of the CMSSM, inasmuch as they enjoy the enhancements due to a light LSP. However, we of course only compare to a single CMSSM element, and one notably chosen in part for its persistent (historical, though no longer) viability against experimental limits.

Conversely, applying the ULTRA:9 cuts to both models, the balance tips decisively in favor of \mathcal{F} - $SU(5)$, whose order of ten-fold absolute enhancement, combined with the order of ten-fold SPS3 absolute suppression, nets a relative visibility advantage of up to 100 times.

It should be clearly remarked, though, that the key point here is not the advantage in discoverability over the SPS3 benchmark itself, since as we have noted it makes very little sense to apply the ULTRA variety of cuts if one is attempting to probe the CMSSM class of models. A much more relevant comparison in this case is the advantage garnered by the ULTRA selection cuts over the CMS selection cuts, holding the No-Scale \mathcal{F} - $SU(5)$ model space constant. As effectively demonstrated by Tables (I,II), this advantage appears to stand remarkably stable, considering the wide range of cross sections considered, near the advertised ratio of order ten. Rather, the key importance of the larger factor demonstrated in Table (III) for comparison of \mathcal{F} - $SU(5)$ against the CMSSM under constant application of the ULTRA:9 cuts is its remarkable ability to differentiate competing explanations for the source of a potential observed signal. Strong differential performance under the ULTRA cutting methodology could then be construed as strong

TABLE III: The ratio of absolute visibility of No-Scale \mathcal{F} - $SU(5)$ versus the CMSSM benchmark SPS3 is tabulated for various collider energies and various cut methodologies. The elements of the \mathcal{F} - $SU(5)$ model space are partitioned for this comparison into light, medium and heavy groupings, according to the mass of the LSP.

\sqrt{s}	CMS : 3	CMS : 6	ULTRA : 6	ULTRA : 9
$m_{\text{LSP}} < 95 \text{ GeV} \quad (\mathcal{F}\text{-A} \dots \mathcal{F}\text{-J})$				
7	1.6	19.5	37.5	317.8
8	1.7	16.3	30.3	176.5
10	1.8	5.5	26.2	88.8
12	1.7	5.8	22.7	74.9
14	1.8	5.4	19.1	59.6
Average	1.7	10.5	27.1	143.5
$95 \text{ GeV} \leq m_{\text{LSP}} < 135 \text{ GeV} \quad (\mathcal{F}\text{-K} \dots \mathcal{F}\text{-O})$				
7	0.0	1.3	0.6	14.4
8	0.1	1.8	0.7	15.1
10	0.1	1.5	1.1	13.2
12	0.1	1.7	1.3	13.4
14	0.1	1.4	1.4	12.0
Average	0.1	1.5	1.0	13.6
$135 \text{ GeV} \leq m_{\text{LSP}} \quad (\mathcal{F}\text{-P} \text{ \& } \mathcal{F}\text{-Q})$				
7	0.00	0.00	0.00	0.01
8	0.00	0.01	0.00	0.02
10	0.00	0.04	0.00	0.06
12	0.00	0.06	0.01	0.10
14	0.00	0.06	0.01	0.14
Average	0.00	0.03	0.00	0.07

evidence that an observed signal could be attributable to a model in the vicinity of the \mathcal{F} - $SU(5)$ universe.

Moving down into the medium weight models of Table (III), we find that the balance shifts. As should be expected, the visibility ratio of \mathcal{F} - $SU(5)$ to SPS3 is up to 100 times higher under the ULTRA:9 cuts than under the CMS:3 cuts. However, rather than parity in the model discovery ratio under the CMS:3 cuts, we find an order of 10 suppression in the absolute visibility of \mathcal{F} - $SU(5)$, and correspondingly, only an order of 10 enhancement under the ULTRA:9 cuts for the \mathcal{F} - $SU(5)$ models in comparison to SPS3. Of course, this is consistent with the observation from Section III that the middle weight and heavy \mathcal{F} - $SU(5)$ models have generally not been ruled out by the CMS:3 cut strategy, while a majority of the lightweight classification has been, along with the SPS3 benchmark itself. The heavy \mathcal{F} - $SU(5)$ points are quite difficult to resolve, even under the ULTRA:9 cuts, as we have advertised previously [11, 12], and will require fulfillment of the promised LHC energy upgrade. The discovery ratios in Table (III) are all substantially less than one for this heavy category, even though, by LSP mass, this is where the SPS3 benchmark belongs. The situation is improved if the heaviest \mathcal{F} - $SU(5)$ point is excluded, but the diffi-

culty in making a direct comparison between competing models is still underscored.

To this point, most of our discussion has focused on the extremes of the selection criteria range, namely the CMS:3 and ULTRA:9 methodologies, we conclude this section with some commentary on the two six jet selection cuts CMS:6 and ULTRA:6, which are in some ways quite similar, *cf.* Table (III), and in some ways distinct, *cf.* Table (I). The absolute discovery advantage of Table (III) would tip in the favor of the light \mathcal{F} - $SU(5)$ models for these cases by a factor of order ten, and the favored middle weight models would exist at basic parity with the CMSSM sample. This is consistent with and complementary to the observation from Table (I) that the CMS:6 cuts are of roughly equal standing with the ULTRA:9 cuts from the CMSSM perspective, although of order ten times worse from the \mathcal{F} - $SU(5)$ perspective, performing in this case comparably to the CMS:3 cuts. Likewise, the ratio ULTRA:6/ULTRA:9 is numerically larger than one, but still of order one for the \mathcal{F} - $SU(5)$ space, and comparatively on the order of ten times smaller when applied to the SPS3 benchmark. For the heavier models, the visibility of the \mathcal{F} - $SU(5)$ models relative to the SPS3 benchmark, although clearly much weaker as a fixed metric, retains the same relative scaling which is apparent for the lighter models, being an order of ten times stronger for either the six jet cut than the CMS:3 cuts, and an order of ten times weaker for either the six jet cut than the ULTRA:9 cut.

If the LHC detector collaborations should shortly release an analysis similar to the selection cuts described here as CMS:6, this would certainly be a step in the right direction, from our point of view. However, it is not immediately clear that this step would in isolation offer a significant improvement over the picture established by the integral jet binning which has already been provided, for example by the CMS collaboration plots reprinted in Figures (1,3). Taken in conjunction, what Tables (I and III) seem to imply is that, while critical to the detectability of No-Scale \mathcal{F} - $SU(5)$, jet count itself is not the only criterion of interest for detection of the No-Scale \mathcal{F} - $SU(5)$ models. In particular, it must be emphasized that not all six-jet (or nine jet or etc.) searches are comparable simply at face value. The question of how and why the two six-jet selection cuts are indeed in some ways so different is the focus of Section (VI).

VI. LESS BECOMES MORE

In this section we emphasize distinctions between the CMS and ULTRA selection cut philosophies which go beyond the obvious shift in the minimal jet count threshold, casting additional light on the dramatic differences which were observed between the two trial six-jet selection cuts discussed in Section (V). Specifically, the remaining differences involve the minimal transverse momentum required for classification as a jet, and a disabling of cuts

on the electromagnetic fraction ratio, the ratio $R(H_T^{\text{miss}})$ of hard to soft jets, and the α_T statistic.

Averaged across the model space, we find that the CMS:3 cuts at $\sqrt{s} = 7$ TeV have a filtering efficacy of 97.6% against the \mathcal{F} - $SU(5)$ signal. This is somewhat disappointing, considering that the sample is composed entirely of the targeted SUSY events. It is an awful lot of gold washing over the pan and down the stream. By comparison, only 91.0% of the SPS3 benchmark was so cut. This suggests strongly that a much more efficiently graded tier of filters must be employed to better differentiate the sand and waste from the few precious nuggets which may pass our way. Digging deeper into the cutting statistics, we find that a full 71.2% of events are cut for not producing at least three jets which satisfy all selection criteria, including the per jet transverse momentum threshold of 50 GeV. Only 1.1% of events are cut for possessing jets which pass the hard momentum threshold while failing either the electromagnetic fraction or pseudo-rapidity limits. The cuts on the leading jet pseudo-rapidity and the transverse momentum of the two leading jets affect 53.8% and 72.9% of all events respectively. The cuts on jet missing energy and the scalar sum of jet transverse momentum net capture rates of 71.1% and 72.1%. Limits on isolated energetic leptons and photons affect 22.5% and 1.5% of events, while the ratio $R(H_T^{\text{miss}})$ acts on 3.9%. The dominant cut, however, is that on α_T , which is active on a total of 92.9% of all events. Even more suggestively, $\alpha_T \geq 0.55$ represents the only cut which has a substantial efficacy as the sole active exclusion on a large number of events, accounting in isolation for the rejection of a full 10.3% of the sample.

It may seem counter intuitive to abandon tried and true techniques which have proven so beneficial for reduction of the SM background against intermediate jet multiplicity events, but we have observed in simulation that, worse even than simply failing to effectively differentiate the ultra-high jet signal, certain of these well known markers may actually preferentially indicate against it [8]. It is worth recalling here that the α_T statistic was originally devised for di-jet processes, and later adapted to multi-jet events by the artful assemblage of two optimized pseudo-jets from the full set of tracks. Its intrinsic relevance for the scaling up to ultra-high jet processes may then be held in some doubt. Indeed, we have observed, *cf.* the upper right plot of Figure Set (2), a rather rapid decline in \mathcal{F} - $SU(5)$ events beyond the value of $\alpha_T = 0.5$. We remind the reader also that the feature of rapid attrition of high jet counts under the $\alpha_T \geq 0.55$ selection cut was particularly relevant to the success of \mathcal{F} - $SU(5)$ in the analysis of Figure (3). In order to better account for these interrelated observations, we now present the formal definition of the jet-based missing energy H_T^{miss} , and also of α_T for multijet events. Likewise, we recall that $H_T \equiv \sum_{\text{jets}} |\vec{p}_T|$ is the simple scalar sum across the magnitudes of the transverse momenta of all

hard jets.

$$H_T^{\text{miss}} \equiv \sqrt{\left(\sum_{\text{jets}} p_T \cos \phi\right)^2 + \left(\sum_{\text{jets}} p_T \sin \phi\right)^2} \quad (2)$$

$$\alpha_T \equiv \frac{1}{2} \left\{ \frac{1 - (\Delta H_T^{\text{MIN}}/H_T)}{1 - (H_T^{\text{miss}}/H_T)^2} \right\} \quad (3)$$

The graphical interpretation of Eq. (2) is that of a vector sum of directed transverse momenta, resulting in an open polygonal shape, whose missing leg gives the magnitude of the missing energy signal. In Eq. (3), ΔH_T is the (positive) difference in the net scalar transverse momentum between two arbitrarily partitioned groupings of the surviving jets. All such possible combinations of pseudo jets are considered, and the minimal value of ΔH_T is employed. If there is no mismeasurement or true missing energy, the value of α_T will just be 1/2. For energy magnitude mismeasurements of otherwise anti-parallel (pseudo) jet pairs, subtraction of the nonvanishing scalar difference ΔH_T will tend to drive α_T below the midline. Note that in this case $\Delta H_T = H_T^{\text{miss}}$, but the squaring of the small (typically $\ll 1$) factor in the denominator renders it less significant. Conversely, genuine missing energy, as manifest in the departure from (pseudo) jet anti-parallelism, will imbalance the vector sum within the factor H_T^{miss} of the denominator more so than the simple magnitude difference ΔH_T , tending to create a contrasting elevation in α_T above one-half.

The central point which explains the failure of the α_T statistic at ultra-high jet multiplicities seems to be that a large availability of relatively soft jets allows for such a wide array of pseudo-jet combinations that it becomes quite likely that a balanced scalar sum $\Delta H_T^{\text{MIN}} \simeq 0$ might be achieved, creating an overall suppression of the α_T value. A very similar attribution may be made for the reason of the (possibly quite experimentally favorable) anomalous bias of $\Delta\phi^*$ toward zero in the \mathcal{F} - $SU(5)$ models, as depicted in the lower left-hand plot of Figure Set (2). Although $\Delta\phi^*$ is not expressly activated in any of the selection criteria described in this work, it remains a statistic of common use and relevance which is designed to establish whether poor scaling of a single jet measurement might be responsible for a false missing energy signature. Specifically, for each surviving jet in turn, $\Delta\phi^i$ registers the absolute azimuthal angle in the range $(0, \pi)$ which separates the transverse momentum vector of the i^{th} jet from the negation of the directional imbalance which arises by omitting that jet from the vector transverse momentum sum. The minimal such value, denoted with the index “*” is the one reported. If a single jet mismeasurement is indeed dominantly responsible for a false missing energy signal, then $\Delta\phi^*$ should register close to zero. However, again, given a wide selection of randomly oriented jets, it becomes in fact quite likely

that the angular orientation of at least one such member might be sufficiently well azimuthally aligned with the true missing energy track that its rescaling could apparently rebalance the event. Visually, we are no longer stretching one leg of an open triangle to make it close to zero length under vector addition and so eliminate the missing energy signal. We are instead perhaps stretching one leg of an open decagon! The α_T selector (and likewise $\Delta\phi^*$) appears simply unsuited for ultra jet searches, and is responsible for a catastrophic signal suppression for the reason described.

If our goal is excavation of the supersymmetric No-Scale \mathcal{F} - $SU(5)$ signal out of the Standard Model rubble, then a critical simultaneous complement to the increased jet multiplicity threshold and elimination of the α_T cut seems to be a lowering of the required transverse momentum per jet. Indeed, even without the α_T cut applied, Figure (1) demonstrates a paucity of ≥ 9 jet events, a fact which we attribute primarily to the large per-jet transverse momentum threshold of $p_T \geq 50$. We have again adopted the aggressive cuts $p_T > 20$ and jets ≥ 9 as the baseline ULTRA selection procedure. There is very recent documentation from the ATLAS collaboration [68] which finds that soft jets below about 20 GeV are not modeled well, with simulations diverging from the actual data. However, above this threshold, the correspondence with data is reported to be quite satisfactory; we find this to be a most affirmative result for our preferred level of selection, which was in some sense designed to target a lower cusp of reasonable efficacy. It is certainly true that a softening of the per-jet momentum threshold will admit into the calculus a significant decentralization from the initial hard scattering intermediate Feynman diagrams. Nevertheless, the basic intuition that fewer hard jets in the early parton level diagrams will yield a correspondingly smaller count of final state soft jets is well confirmed by the Monte Carlo, and we have demonstrated not only a readily detectable signal for No-Scale \mathcal{F} - $SU(5)$ above the SM background, but also a clear differentiation between No-Scale \mathcal{F} - $SU(5)$ and a typical competing post-SM scenario. The unique SUSY mass hierarchy of No-Scale \mathcal{F} - $SU(5)$, which we have not found replicated by any models of the CMSSM variety, convinces us of the broad generality of these conclusions.

Aware of these considerations, it is worth remarking that some caution is in order to ensure that this same principle in reverse does not undermine the missing energy measurement itself at high jet multiplicities. Again, our Monte Carlo indicates, despite a strong likelihood that the prior concern does play some role in the simulation, that the ULTRA:9 cuts based on jet multiplicity, pseudo rapidity per jet, transverse momentum p_T per jet, the net jet energy H_T , and the net jet missing energy H_T^{miss} do provide striking differentiation of the No-Scale \mathcal{F} - $SU(5)$ models above the competing SM background, and also with respect to competing mSUGRA/CMSSM proposals. The need for extra suppression of backgrounds, a task frequently assigned to selections based on

α_T , is here circumvented by the simple observation that the ultra-high jet threshold itself accomplishes an extraordinarily robust suppression of the Standard Model. Indeed, it seems in this case, that less can amount to more.

VII. EXCAVATING SUSY WITH A 1.1 fb⁻¹ LHC

The $t\bar{t}$ + jets background is certainly not sufficient to model the detector response under the CMS style three jet selection criteria, nor for the two considered six jet scenarios. As elaborated in Section (III), this had been a consideration in our decision to focus in the present work on relative rather than absolute performance metrics, such as the comparative visibility advantage garnered by the No-Scale \mathcal{F} - $SU(5)$ model class under application of the ULTRA:9 cutting scenario versus the CMS:3 scenario. We argued that some cancellation in this ratio between additional contributions to the SM backgrounds should be expected, but that the weaker performance at high jet multiplicities of those SM background components which have been neglected in simulation implies that the reported ten-fold visibility advantage is in actuality a lower bound. In the present section, we attempt to quantify the factor by which the discovery advantage of the ULTRA selection cut criteria within the No-Scale \mathcal{F} - $SU(5)$ model space may be enhanced.

Table (IV) represents a variation on the Table (I) theme, again comparing single model visibility relative to the application of various cuts. We reduce the cutting scenarios, though, to only the CMS:3 and ULTRA:9 styles, and the collider energy to only $\sqrt{s} = 7$ TeV. The reason for this is that in Table (IV) we wish to apply certain more concrete values of the low jet background, taken directly from experiment. For this purpose, we will extrapolate from graphical backgrounds presented for 1.1 pb⁻¹ of CMS data [1]. This translates in the present context to a value of about 195 observations for 1 fb⁻¹ of data. We are assuming still adequate background suppression under the ULTRA:9 cuts for all but our $t\bar{t}$ + jets simulation. Given actual data for the intermediate jet multiplicity cuts, we now add to the Table (I) presentation a printing of the absolute discovery index N , *i.e.* the projected number of inverse femtobarns of luminosity which would need to be integrated in order to achieve a value of five for the signal visibility metric $S/\sqrt{B+1}$.

The extraordinarily rapid scaling of the discovery index N with the LSP mass, *cf.* Refs. [11, 12], which is basically collinear with the primary input parameter $M_{1/2}$, highlights the comparative stability of the relative advantage garnered under the ULTRA:9 selection cuts, as compared to the more standard CMS:3 variety. Moreover, the rather small absolute values of N which exist for the ULTRA:9 selection cuts up to a level of about $m_{\text{LSP}} \simeq 110$ GeV, *i.e.* the vicinity of our leading benchmark \mathcal{F} -N, strikingly exemplifies our claim that the vast

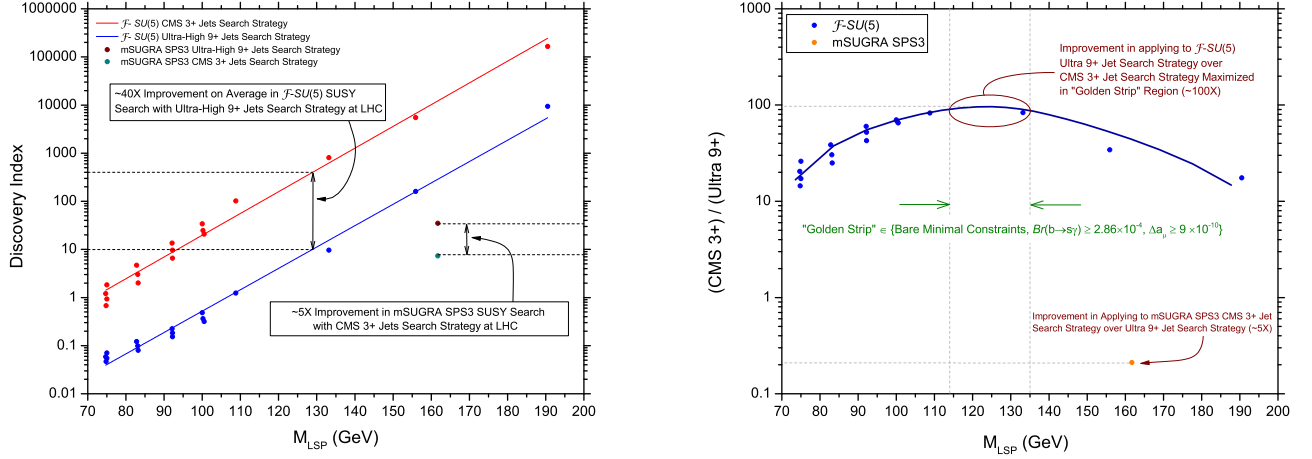


FIG. 6: The lefthand figure plots the absolute discovery index N of the No-Scale \mathcal{F} -SU(5) model space, *i.e.* the projected number of inverse femtobarns of luminosity which would need to be integrated in order to achieve a value of five for the signal visibility metric $S/\sqrt{B+1}$. The backgrounds under the CMS:3 cuts are extracted from a CMS analysis [1] to a value of about 195 observations for 1 fb^{-1} of data. The backgrounds under the ULTRA:9 cuts are from our simulation of $t\bar{t}$ + jets processes. The right-hand figure demonstrates the distribution of the ULTRA:9 discovery advantage as a function of the LSP mass. Curiously, the ratio is maximized nearest to the most experimentally favored region, which consists of satisfaction of the experimental limits on contributions to the anomalous magnetic moment of the muon $(g-2)_\mu$ and the branching ratio of the flavor changing neutral current process $(b \rightarrow s\gamma)$, over and above the bare-minimal constraints of [9]. We define this region to constitute a new “Golden Strip” within the bare-minimally constrained [9] No-Scale \mathcal{F} -SU(5) model space.

majority of the No-Scale \mathcal{F} -SU(5) parameter space is already fully testable under the existing accumulation of data. The most striking result of this tabulation, however, is the dramatic enhancement of the relative visibility, which jumps from order ten in Table (I), to up to order of one hundred in the present context. This assumes, again, a sufficient modeling of the ultra-high jet multiplicity SM backgrounds by the $t\bar{t}$ + jets processes, a topic which will itself be revisited in Section (VIII) following.

The results of Table (IV) are translated into graphical form in Figure Set (6), with the absolute discovery indices plotted on the left, and the per-model comparative discovery ratio plotted on the right. The disconnect between the continuity embodied in the No-Scale \mathcal{F} -SU(5) model space and the island CMSSM model SPS3 highlights the difficulty of a head to head comparison between models with fundamentally different origins and spectra. Of course, the fact that SPS3 fares “better” in terms of discoverability at a corresponding LSP mass is consistent with the fact that this model has already been ruled out. Because of the distinctively light gluino and stop squark in No-Scale \mathcal{F} -SU(5), much lighter than all other squarks, these models tend to be much more resilient against light squark limits than CMSSM models with comparably light LSP particles, and comparably strong SUSY production cross sections.

Curiously, the plot of the comparative discovery ratio demonstrates that the relative advantage of the ULTRA:9 cutting philosophy is in fact maximized, reaching an extrapolated peak of about 100 times, in the immediate vicinity of model elements which were favored

in our Section (III) analysis of the most recent LHC data. This region will be taken to constitute a newly updated “Golden Strip” (*cf.* Ref [4]) of the bare minimally constrained [9] model space. The region of the Golden Strip features an exceedingly satisfactory phenomenological agreement with limits on the flavor changing neutral current $(b \rightarrow s\gamma)$ process, using a two standard deviation lower bound of 2.86×10^{-4} on $Br(b \rightarrow s\gamma)$ [69, 70], and likewise with limits on the anomalous magnetic moment of the muon, using a lower bound on the post-SM contribution Δa_μ to $(g-2)_\mu \div 2$ of 11×10^{-10} [71], or more conservatively, of 9×10^{-10} . Although both considered effects are at their lower limits at the strip boundary, they exert pressure in opposing directions on m_{LSP} (or $M_{1/2}$) due to the fact that the leading SUSY contributions to $Br(b \rightarrow s\gamma)$ enter with an opposing sign to the SM term (requiring a sufficiently large mass that they not undo the SM component), while for the non-SM contribution to Δa_μ , the effect is additive (requiring a sufficiently small mass to make an appreciable contribution).

The complete \mathcal{F} -SU(5) model space is further easily consistent with the process $B_s^0 \rightarrow \mu^+ \mu^-$, using an upper bound on the branching ratio of 1.9×10^{-8} [51]. Collider based studies [72] of this process are expected to continue to compete well with direct detection searches for this process, and place rather stringent limits on certain sectors of the CMSSM. However, these limits ease with decreasing $\tan \beta$, with an extremely strong dependence in the sixth power. No-Scale \mathcal{F} -SU(5) stably predicts a comparatively small ratio for $\tan \beta$, in the vicinity of the value 20, which should not be impinged upon by any near term studies. Likewise, our rather heavy CP-Odd Higgs

TABLE IV: An extension of the Table (I) analysis is carried out for the seventeen \mathcal{F} - $SU(5)$ benchmarks, as well as the CMSSM representative SPS3. The collider energy represented is constant at $\sqrt{s} = 7$ TeV. The backgrounds under the CMS:3 cuts are extracted from a CMS analysis [1] to a value of about 195 observations for 1 fb^{-1} of data. The backgrounds under the ULTRA:9 cuts are from our simulation of $t\bar{t}$ + jets processes. Since the backgrounds are better known here than was generally true in Table (I), we are comfortable printing the absolute discovery index N , *i.e.* the projected number of inverse femtobarns of luminosity which would need to be integrated in order to achieve a value of five for the signal visibility metric $S/\sqrt{B+1}$, for each model under the CMS:3 and ULTRA:9 cuts, in addition to the discovery ratio of the two procedures. However, because of the strong model dependence, we suppress presentation of an average for these columns. This data is represented in graphical form by Figure Set (6).

Model	$N(\text{CMS:3})$	$N(\text{ULTRA:9})$	$\frac{N(\text{CMS:3})}{N(\text{ULTRA:9})}$
\mathcal{F} -A	0.7	0.05	14.5
\mathcal{F} -B	0.9	0.05	17.2
\mathcal{F} -C	1.2	0.06	20.5
\mathcal{F} -D	1.8	0.07	26.1
\mathcal{F} -E	2.0	0.08	25.0
\mathcal{F} -F	3.0	0.10	30.5
\mathcal{F} -G	4.7	0.12	38.7
\mathcal{F} -H	6.6	0.15	42.7
\mathcal{F} -I	9.6	0.18	52.2
\mathcal{F} -J	13.6	0.23	60.1
\mathcal{F} -K	20.8	0.32	65.2
\mathcal{F} -L	24.7	0.36	67.9
\mathcal{F} -M	34.2	0.49	70.3
\mathcal{F} -N	102.3	1.23	82.9
\mathcal{F} -O	808.5	9.7	83.5
\mathcal{F} -P	5.49×10^3	160.1	34.3
\mathcal{F} -Q	1.66×10^5	9.45×10^3	17.5
\mathcal{F} -Average	—	—	44.1
SPS3	7.3	34.8	0.2

A, with M_A in the range of $0.6 - 1.6$ TeV, contributes to a persistent immunity against this metric. We emphasize that the heavy squarks of these models, having a mass of about 1 TeV, preserve the defining intent of SUSY with respect to naturalness in stabilization of the gauge hierarchy.

The LSP within the full No-Scale \mathcal{F} - $SU(5)$ model space is also quite satisfactory with regards to the relevant spin-independent scattering cross-section bounds on Weakly Interacting Massive Particles (WIMPs) from direct detection probes from XENON100 [52], and spin-dependent scattering cross-section limits from Super Kamiokande [53], escaping the spin-dependent limits by three to four orders of magnitude. This is facilitated, for the latter case in particular, by the fact that our mod-

els are in the stau-LSP neutralino coannihilation region, with relatively heavy squark content. The status of the Higgs boson search is also currently getting quite interesting, with Summer conference reports from the ATLAS collaboration indicating potential signals at about the 2.8σ level peaking around 128 GeV and 144 GeV, and from the CMS collaboration indicating potential signals at about the 2.0σ level peaking around 120 GeV and 140 GeV. The light Higgs in a large region of the \mathcal{F} - $SU(5)$ model space is predicted to have a mass of 120-128 GeV. We note also here that the vector-like particle mass M_V , which may take a value up to several TeV, and which does not directly couple to the Higgs, should make a comparatively minor contribution to the Higgs mass. A potentially relevant study of the general correlation between the Higgs and a vector-like field multiplet has recently been released [73][74].

VIII. ELABORATION ON STANDARD MODEL BACKGROUNDS

Considering the large number of hadronic jets which are required by our optimized ultra-high jet signatures, we have argued [7, 8] that there is little intrusion from SM background processes after post-processing cuts. Specifically, we have examined the background processes studied in [67, 75] and assessed the relevance of each to our model in the initial LHC run. Our conclusion to date has been that only the $t\bar{t}$ + jets process possesses the requisite minimum cross-section and multiplicity of final state jet production to compete with the \mathcal{F} - $SU(5)$ signal. Processes with a larger number of top quarks can also generate events with a large number of jets, however, the cross-sections have been deemed sufficiently suppressed to be negligible, bearing in mind the large number of ultra-high jet events which our model will generate. Similarly, we have neglected in our Monte Carlo the pure QCD (2, 3, 4) jet events, one or more vector boson events, and all $b\bar{b}$ processes, since none of these have been judged capable of sufficient event production with 9 or more jets after post-processing cuts have been applied. The same has been taken to hold for those more complicated background processes involving combinations of top quarks, jets, and one or more vector bosons, which yield a very large number of raw events, though it has been expected that practically all of the jets from detector effects beyond the initial hadronization would be ultimately discarded. We revisit these conclusions in the present section, and in particular, consider the expected consequences for discoverability of our model if these assumptions should be in various regards materially incorrect or incomplete.

It is not immediately clear how the published CMS results for ≥ 9 jets with $p_T \geq 50$ GeV translates into the context of a reduced threshold on the transverse momentum p_T , and we shall continue to study the issue. It seems for now though that we can set limits based on a set of

worst case assumptions, comparing the CMS results with our own $t\bar{t}$ + jets simulation. Following this lead, if we scale the QCD multijet background at three times the combined $t\bar{t}, W^\pm, Z$ + jets contribution in Figure (1), of which nearly all is taken to be modeled by $t\bar{t}$ + jets in the Ultra-High jet regime, the net result is a 4 times upgrade of the background. This reduces the average discovery advantage $N(\text{ULTRA} : 9)/N(\text{CMS} : 3)$ from the value of 44.1 given in Table (IV) to a value of 15.4; perhaps not so surprisingly, this is essentially the titular result of order ten from Table (IV), based on a naïve global application of just the $t\bar{t}$ + jets sampling. If we assume the combined $t\bar{t}, W^\pm, Z$ + jets contribution is only 25% modeled by the $t\bar{t}$ + jets, then a multiplicative factor of 16.0 is applied to the backgrounds, and the ULTRA:9 discovery advantage is still a healthy 4.1.

IX. CONCLUSION AND SUMMARY

We seem now to be firmly entering the golden age of LHC physics. The collider is working brilliantly, and exceeding scheduled goals for the ramping up of integrated luminosity. By recently crossing the threshold of one delivered femtobarn of integrated luminosity, this remarkable machine begins to dramatically reshape our perceptions of the plausible landscape of Supersymmetric extensions to the Standard Model, upgrading the initial reports based upon only 35 pb^{-1} of integrated luminosity by more than 30 times. The present work marks our first opportunity to comment on the ongoing LHC search following the first presented analysis [1] of data eclipsing the 1.1 fb^{-1} milestone, but likewise extends the scope of prior work in several other regards. In particular, we have combined an established Monte Carlo simulation of the full bare minimal parameter space of the No-Scale \mathcal{F} - $SU(5)$ model class, at five distinct collider energies with the recently introduced discovery index statistic N , for four specific cut methodologies, two of which are considered for the first time. In addition, we supplement our limited background simulation with actual collider results harvested from the most recent LHC observations.

Several new key results have emerged during the current study. We have established the first exclusion boundaries on the bare-minimally constrained model space of No-Scale \mathcal{F} - $SU(5)$, resulting from the first 1.1 inverse femtobarns of integrated LHC luminosity. We find that the LSP mass in these models should be at least about 92 GeV, with a corresponding boundary gaugino mass $M_{1/2}$ above about 485 GeV, as characterized by the benchmark \mathcal{F} -J. We find the optimal fit to occur at somewhat heavier models, including a very suitable benchmark located at $m_{\text{LSP}} = 108.8 \text{ GeV}$ and $M_{1/2} = 560 \text{ GeV}$, named \mathcal{F} -N. Furthermore, in contrast to higher mass constraints in the CMSSM, we found lower limits on the gluino and heavy squark masses in the \mathcal{F} - $SU(5)$ model space in the range of 658-674 GeV and 854-1088 GeV, respectively, with the minimum bound-

ary on the light stop mass at about 520 GeV. Not only are the models in the vicinity of these points capable of adroitly escaping the onslaught of LHC data which is currently decimating the standard mSUGRA/CMSSM benchmarks, they are also able to efficiently explain certain tantalizing production excesses over the SM background which have been reported by the CMS collaboration. Critically also, a clear path is provided to salvage the defining motivation of Supersymmetry itself, that being a natural stabilization of the gauge hierarchy, as embodied in sparticle mass splittings of not more than about 1 TeV.

We have emphasized throughout the simple but rather critical observation that different model classifications respond differently to various alternative selection cut criteria. In particular, results which legitimately discount substantial segments of the Minimally Constrained Supersymmetric Standard Model must not be inferred to also do similar damage to the underlying framework of Supersymmetry itself. This is because: 1) the CMSSM represents a simplification which is sometimes necessary for the convenience of the analyst, but perhaps not so for nature herself; 2) it is simply quite difficult to make fair comparisons between contending models – one might say after all that this is why they are in fact called different models; and 3) again, critically, any subtle reordering of the model spectra may translate to substantially differential signal responses to the chosen selection cuts. Highlighting these observations, we have here expanded our study of a proposed set of selection cuts designed to reveal the natural ultra-high jet multiplicity signal associated with the stable mass hierarchy $m_{\tilde{t}} < m_{\tilde{g}} < m_{\tilde{q}}$ of the \mathcal{F} - $SU(5)$ models. It has been demonstrated that an enhancement of order ten in model visibility may be attained by adoption of these cuts, which is remarkably stable in simulation across the \mathcal{F} - $SU(5)$ model space, and likewise also for a sampling of various upgraded LHC beam energies. This factor is sufficient to immediately and definitively test a majority of the No-Scale \mathcal{F} - $SU(5)$ model space, using only the already collected LHC data set.

We have stressed that habits established in lower jet multiplicity searches with regards to the appropriate kinematic thresholds per jet and missing energy diagnostics such as α_T and $\Delta\phi^*$ do not necessarily translate well into the ultra-high jet multiplicity search regime. The extraordinary cost, both of labor and capital, exerted thus far in the LHC effort argue vigorously that every available efficiency which may be freely rendered from updates in the methods of analysis should be promptly seized up. As the long-favored oases of the CMSSM framework evaporate before our eyes, the time approaches rapidly when alternative search criteria must be implemented, designed to uniquely illuminate new dreams within the broader SUSY philosophy. The extraordinary potential discoverability of No-Scale \mathcal{F} - $SU(5)$, apparent though only under application of the appropriate selection tool, is at the heart of our claim to a model representing the dichotomy

of imminent testability combined with a remarkable resilience of viability in the face of all existing testing.

Acknowledgments

This research was supported in part by the DOE grant DE-FG03-95-Er-40917 (TL and DVN), by the Nat-

ural Science Foundation of China under grant numbers 10821504 and 11075194 (TL), by the Mitchell-Heep Chair in High Energy Physics (JAM), and by the Sam Houston State University 2011 Enhancement Research Grant program (JWW). We also thank Sam Houston State University for providing high performance computing resources.

-
- [1] “Search for supersymmetry in all-hadronic events with α_T ,” (2011), CMS PAS SUS-11-003, URL <http://cdsweb.cern.ch/record/1370596>.
 - [2] A. Strumia, “Implications of first LHC results,” (2011), 1107.1259.
 - [3] T. Li, J. A. Maxin, D. V. Nanopoulos, and J. W. Walker, “The Golden Point of No-Scale and No-Parameter \mathcal{F} - $SU(5)$,” Phys. Rev. **D83**, 056015 (2011), 1007.5100.
 - [4] T. Li, J. A. Maxin, D. V. Nanopoulos, and J. W. Walker, “The Golden Strip of Correlated Top Quark, Gaugino, and Vectorlike Mass In No-Scale, No-Parameter \mathcal{F} - $SU(5)$,” Phys. Lett. **B699**, 164 (2011), 1009.2981.
 - [5] T. Li, J. A. Maxin, D. V. Nanopoulos, and J. W. Walker, “Super No-Scale \mathcal{F} - $SU(5)$: Resolving the Gauge Hierarchy Problem by Dynamic Determination of $M_{1/2}$ and $\tan\beta$,” (2010), 1010.4550.
 - [6] T. Li, J. A. Maxin, D. V. Nanopoulos, and J. W. Walker, “Blueprints of the No-Scale Multiverse at the LHC,” (2011), 1101.2197.
 - [7] T. Li, J. A. Maxin, D. V. Nanopoulos, and J. W. Walker, “Ultra High Jet Signals from Stringy No-Scale Supergravity,” (2011), 1103.2362.
 - [8] T. Li, J. A. Maxin, D. V. Nanopoulos, and J. W. Walker, “The Ultra-High Jet Multiplicity Signal of Stringy No-Scale \mathcal{F} - $SU(5)$ at the $\sqrt{s} = 7$ TeV LHC,” (2011), 1103.4160.
 - [9] T. Li, J. A. Maxin, D. V. Nanopoulos, and J. W. Walker, “The Unification of Dynamical Determination and Bare Minimal Phenomenological Constraints in No-Scale \mathcal{F} - $SU(5)$,” (2011), 1105.3988.
 - [10] T. Li, J. A. Maxin, D. V. Nanopoulos, and J. W. Walker, “The Race for Supersymmetric Dark Matter at XENON100 and the LHC: Stringy Correlations from No-Scale \mathcal{F} - $SU(5)$,” (2011), 1106.1165.
 - [11] T. Li, J. A. Maxin, D. V. Nanopoulos, and J. W. Walker, “A Two-Tiered Correlation of Dark Matter with Missing Transverse Energy: Reconstructing the Lightest Supersymmetric Particle Mass at the LHC,” (2011), 1107.2375.
 - [12] T. Li, J. A. Maxin, D. V. Nanopoulos, and J. W. Walker, “Prospects for Discovery of Supersymmetric No-Scale \mathcal{F} - $SU(5)$ at The Once and Future LHC,” (2011), 1107.3825.
 - [13] S. M. Barr, “A New Symmetry Breaking Pattern for $SO(10)$ and Proton Decay,” Phys. Lett. **B112**, 219 (1982).
 - [14] J. P. Derendinger, J. E. Kim, and D. V. Nanopoulos, “Anti- $SU(5)$,” Phys. Lett. **B139**, 170 (1984).
 - [15] I. Antoniadis, J. R. Ellis, J. S. Hagelin, and D. V. Nanopoulos, “Supersymmetric Flipped $SU(5)$ Revitalized,” Phys. Lett. **B194**, 231 (1987).
 - [16] J. Jiang, T. Li, and D. V. Nanopoulos, “Testable Flipped $SU(5) \times U(1)_X$ Models,” Nucl. Phys. **B772**, 49 (2007), hep-ph/0610054.
 - [17] J. Jiang, T. Li, D. V. Nanopoulos, and D. Xie, “ \mathcal{F} - $SU(5)$,” Phys. Lett. **B677**, 322 (2009).
 - [18] J. Jiang, T. Li, D. V. Nanopoulos, and D. Xie, “Flipped $SU(5) \times U(1)_X$ Models from F-Theory,” Nucl. Phys. **B830**, 195 (2010), 0905.3394.
 - [19] T. Li, D. V. Nanopoulos, and J. W. Walker, “Elements of F-fast Proton Decay,” Nucl. Phys. **B846**, 43 (2011), 1003.2570.
 - [20] T. Li, J. A. Maxin, D. V. Nanopoulos, and J. W. Walker, “Dark Matter, Proton Decay and Other Phenomenological Constraints in \mathcal{F} - $SU(5)$,” Nucl. Phys. **B848**, 314 (2011), 1003.4186.
 - [21] E. Cremmer, S. Ferrara, C. Kounnas, and D. V. Nanopoulos, “Naturally Vanishing Cosmological Constant in $N = 1$ Supergravity,” Phys. Lett. **B133**, 61 (1983).
 - [22] J. R. Ellis, A. B. Lahanas, D. V. Nanopoulos, and K. Tamvakis, “No-Scale Supersymmetric Standard Model,” Phys. Lett. **B134**, 429 (1984).
 - [23] J. R. Ellis, C. Kounnas, and D. V. Nanopoulos, “Phenomenological $SU(1,1)$ Supergravity,” Nucl. Phys. **B241**, 406 (1984).
 - [24] J. R. Ellis, C. Kounnas, and D. V. Nanopoulos, “No Scale Supersymmetric Guts,” Nucl. Phys. **B247**, 373 (1984).
 - [25] A. B. Lahanas and D. V. Nanopoulos, “The Road to No Scale Supergravity,” Phys. Rept. **145**, 1 (1987).
 - [26] J. R. Ellis, J. Hagelin, D. V. Nanopoulos, and K. Tamvakis, “Weak Symmetry Breaking by Radiative Corrections in Broken Supergravity,” Phys. Lett. **B125**, 275 (1983).
 - [27] J. R. Ellis, S. Kelley, and D. V. Nanopoulos, “Precision LEP data, supersymmetric GUTs and string unification,” Phys. Lett. **B249**, 441 (1990).
 - [28] J. R. Ellis, S. Kelley, and D. V. Nanopoulos, “Probing the desert using gauge coupling unification,” Phys. Lett. **B260**, 131 (1991).
 - [29] U. Amaldi, W. de Boer, and H. Furstenau, “Comparison of grand unified theories with electroweak and strong coupling constants measured at LEP,” Phys. Lett. **B260**, 447 (1991).
 - [30] P. Langacker and M.-X. Luo, “Implications of precision electroweak experiments for M_t , ρ_0 , $\sin^2\theta_W$ and grand unification,” Phys. Rev. **D44**, 817 (1991).
 - [31] F. Anselmo, L. Cifarelli, A. Peterman, and A. Zichichi, “The Effective experimental constraints on $M(\text{SUSY})$ and $M(\text{GUT})$,” Nuovo Cim. **A104**, 1817 (1991).
 - [32] F. Anselmo, L. Cifarelli, A. Peterman, and A. Zichichi, “The Convergence of the gauge couplings at $E(\text{GUT})$ and above: Consequences for $\alpha_3(M(Z))$ and SUSY breaking,” Nuovo Cim. **A105**, 1025 (1992).

- [33] G. Costa, J. R. Ellis, G. L. Fogli, D. V. Nanopoulos, and F. Zwirner, “Neutral Currents Within and Beyond the Standard Model,” Nucl. Phys. **B297**, 244 (1988).
- [34] J. L. Lopez and D. V. Nanopoulos, “A New scenario for string unification,” Phys.Rev.Lett. **76**, 1566 (1996), hep-ph/9511426.
- [35] J. R. Ellis, J. S. Hagelin, D. V. Nanopoulos, and M. Srednicki, “Search for Supersymmetry at the anti-p p Collider,” Phys. Lett. **B127**, 233 (1983).
- [36] J. R. Ellis, J. S. Hagelin, D. V. Nanopoulos, K. A. Olive, and M. Srednicki, “Supersymmetric relics from the big bang,” Nucl. Phys. **B238**, 453 (1984).
- [37] H. Goldberg, “Constraint on the photino mass from cosmology,” Phys. Rev. Lett. **50**, 1419 (1983).
- [38] M. Gell-Mann, P. Ramond, and R. Slansky, in *Supergravity*, edited by F. van Nieuwenhuizen and D. Freedman (North Holland, Amsterdam, 1979), p. 315.
- [39] T. Yanagida, in *Proceedings of the Workshop on Unified Field Theory and Baryon Number of the Universe* (KEK, Japan, 1979).
- [40] H. Georgi and D. V. Nanopoulos, “Ordinary Predictions from Grand Principles: T Quark Mass in $O(10)$,” Nucl. Phys. **B155**, 52 (1979).
- [41] C. Beasley, J. J. Heckman, and C. Vafa, “GUTs and Exceptional Branes in F-theory - I,” JHEP **01**, 058 (2009), 0802.3391.
- [42] C. Beasley, J. J. Heckman, and C. Vafa, “GUTs and Exceptional Branes in F-theory - II: Experimental Predictions,” JHEP **01**, 059 (2009), 0806.0102.
- [43] A. Font and L. Ibanez, “Yukawa Structure from $U(1)$ Fluxes in F-theory Grand Unification,” JHEP **0902**, 016 (2009), 0811.2157.
- [44] C.-M. Chen and Y.-C. Chung, “A Note on Local GUT Models in F-Theory,” Nucl.Phys. **B824**, 273 (2010), 0903.3009.
- [45] T. Li, “ $SU(5)$ and $SO(10)$ Models from F-Theory with Natural Yukawa Couplings,” Phys.Rev. **D81**, 065018 (2010), 0905.4563.
- [46] J. R. Ellis, D. V. Nanopoulos, and K. A. Olive, “Lower limits on soft supersymmetry breaking scalar masses,” Phys. Lett. **B525**, 308 (2002), arXiv:0109288.
- [47] J. Ellis, A. Mustafayev, and K. A. Olive, “Resurrecting No-Scale Supergravity Phenomenology,” Eur. Phys. J. **C69**, 219 (2010), 1004.5399.
- [48] E. Komatsu et al. (WMAP), “Seven-Year Wilkinson Microwave Anisotropy Probe (WMAP) Observations: Cosmological Interpretation,” Astrophys.J.Suppl. **192**, 18 (2010), 1001.4538.
- [49] R. Barate et al. (LEP Working Group for Higgs boson searches), “Search for the standard model Higgs boson at LEP,” Phys. Lett. **B565**, 61 (2003), hep-ex/0306033.
- [50] W. M. Yao et al. (Particle Data Group), “Review of Particle physics,” J. Phys. **G33**, 1 (2006).
- [51] S. C. et al. [CMS Collaboration], “Search for $B_s^0 \rightarrow \mu^+ \mu^-$ and $B^0 \rightarrow \mu^+ \mu^-$ decays in pp collisions at $\sqrt{s} = 7$ TeV,” (2011), 1107.5834.
- [52] E. Aprile et al. (XENON100), “Dark Matter Results from 100 Live Days of XENON100 Data,” (2011), 1104.2549.
- [53] T. Tanaka et al. (Kamiokande), “An Indirect Search for WIMPs in the Sun using 3109.6 days of upward-going muons in Super-Kamiokande,” (2011), 1108.3384.
- [54] V. Khachatryan et al. (CMS Collaboration), “Search for Supersymmetry in pp Collisions at 7 TeV in Events with Jets and Missing Transverse Energy,” Phys.Lett. **B698**, 196 (2011), 1101.1628.
- [55] “Search strategy for exclusive multi-jet events from supersymmetry at CMS,” (2009), CMS PAS SUS-09-001, URL <http://cdsweb.cern.ch/record/1194509>.
- [56] B. C. Allanach et al., “The Snowmass points and slopes: Benchmarks for SUSY searches,” Eur. Phys. J. **C25**, 113 (2002), hep-ph/0202233.
- [57] T. Stelzer and W. F. Long, “Automatic generation of tree level helicity amplitudes,” Comput. Phys. Commun. **81**, 357 (1994), hep-ph/9401258.
- [58] J. Alwall et al., “MadGraph/MadEvent Collider Event Simulation Suite,” (2011), URL <http://madgraph.hep.uiuc.edu/>.
- [59] J. Alwall et al., “MadGraph/MadEvent v4: The New Web Generation,” JHEP **09**, 028 (2007), 0706.2334.
- [60] T. Sjostrand, S. Mrenna, and P. Z. Skands, “PYTHIA 6.4 Physics and Manual,” JHEP **05**, 026 (2006), hep-ph/0603175.
- [61] J. Conway et al., “PGS4: Pretty Good (Detector) Simulation,” (2009), URL <http://www.physics.ucdavis.edu/~conway/research/>.
- [62] T. Li, J. A. Maxin, D. V. Nanopoulos, and J. W. Walker, “CutLHCO: A Tool For Detector Selection Cuts,” (2011), URL http://www.joelwalker.net/code/cut_lhco.tar.gz.
- [63] G. Belanger, F. Boudjema, A. Pukhov, and A. Semenov, “Dark matter direct detection rate in a generic model with micrOMEGAs2.1,” Comput. Phys. Commun. **180**, 747 (2009), 0803.2360.
- [64] A. Djouadi, J.-L. Kneur, and G. Moultaka, “SuSpect: A Fortran code for the supersymmetric and Higgs particle spectrum in the MSSM,” Comput. Phys. Commun. **176**, 426 (2007), hep-ph/0211331.
- [65] ATLAS, “Measurement of multi-jet cross sections in proton-proton collisions at a 7 TeV center-of-mass energy,” (2011), 1107.2092.
- [66] S. Chatrchyan et al. (CMS Collaboration), “Search for Three-Jet Resonances in pp Collisions at $\sqrt{s} = 7$ TeV,” (2011), 1107.3084.
- [67] H. Baer, V. Barger, A. Lessa, and X. Tata, “Capability of LHC to discover supersymmetry with $\sqrt{s} = 7$ TeV and 1 fb^{-1} ,” JHEP **06**, 102 (2010), 1004.3594.
- [68] G. Aad et al. (ATLAS), “Properties of jets measured from tracks in proton-proton collisions at center-of-mass energy $\sqrt{s} = 7$ TeV with the ATLAS detector,” (2011), 1107.3311.
- [69] E. Barberio et al. (Heavy Flavor Averaging Group (HFAG)), “Averages of b -hadron properties at the end of 2006,” (2007), 0704.3575.
- [70] M. Misiak et al., “The first estimate of $\text{Br}(\bar{B} \rightarrow X_s \gamma)$ at $\mathcal{O}(\alpha_s^2)$,” Phys. Rev. Lett. **98**, 022002 (2007), hep-ph/0609232.
- [71] G. W. Bennett et al. (Muon g-2), “Measurement of the negative muon anomalous magnetic moment to 0.7-ppm,” Phys. Rev. Lett. **92**, 161802 (2004), hep-ex/0401008.
- [72] A. Akrotyd, F. Mahmoudi, and D. Santos, “The decay $B_s \rightarrow \mu^+ \mu^-$: updated SUSY constraints and prospects,” (2011), 1108.3018.
- [73] T. Li, J. A. Maxin, D. V. Nanopoulos, and J. W. Walker (2011), in Preparation.
- [74] J. L. Evans, M. Ibe, and T. T. Yanagida, “Probing Extra Matter in Gauge Mediation Through the Lightest Higgs Boson Mass,” (2011), 1108.3437.

- [75] B. Altunkaynak, M. Holmes, P. Nath, B. D. Nelson, and G. Peim, “SUSY Discovery Potential and Benchmarks for Early Runs at $\sqrt{s} = 7$ TeV at the LHC,” *Phys. Rev. D* **82**, 115001 (2010), 1008.3423.